Gear Expo '89 PRESHOW

GEAR TECHNOLOGY

The Journal of Gear Manufacturing

JULY/AUGUST 1989

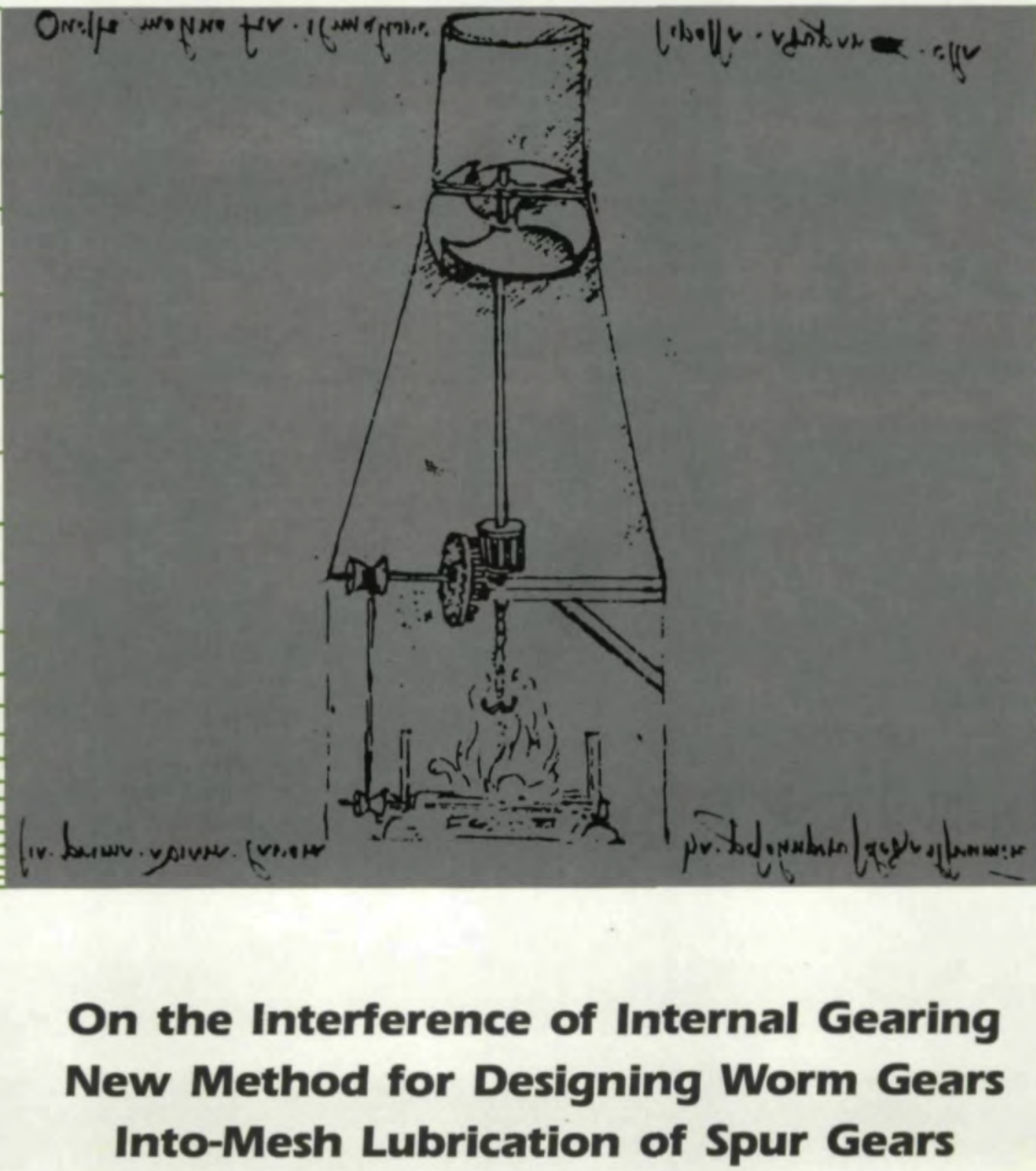

On the Interference of Internal Gearing
New Method for Designing Worm Gears
Into-Mesh Lubrication of Spur Gears
Estimating Hobbing Times

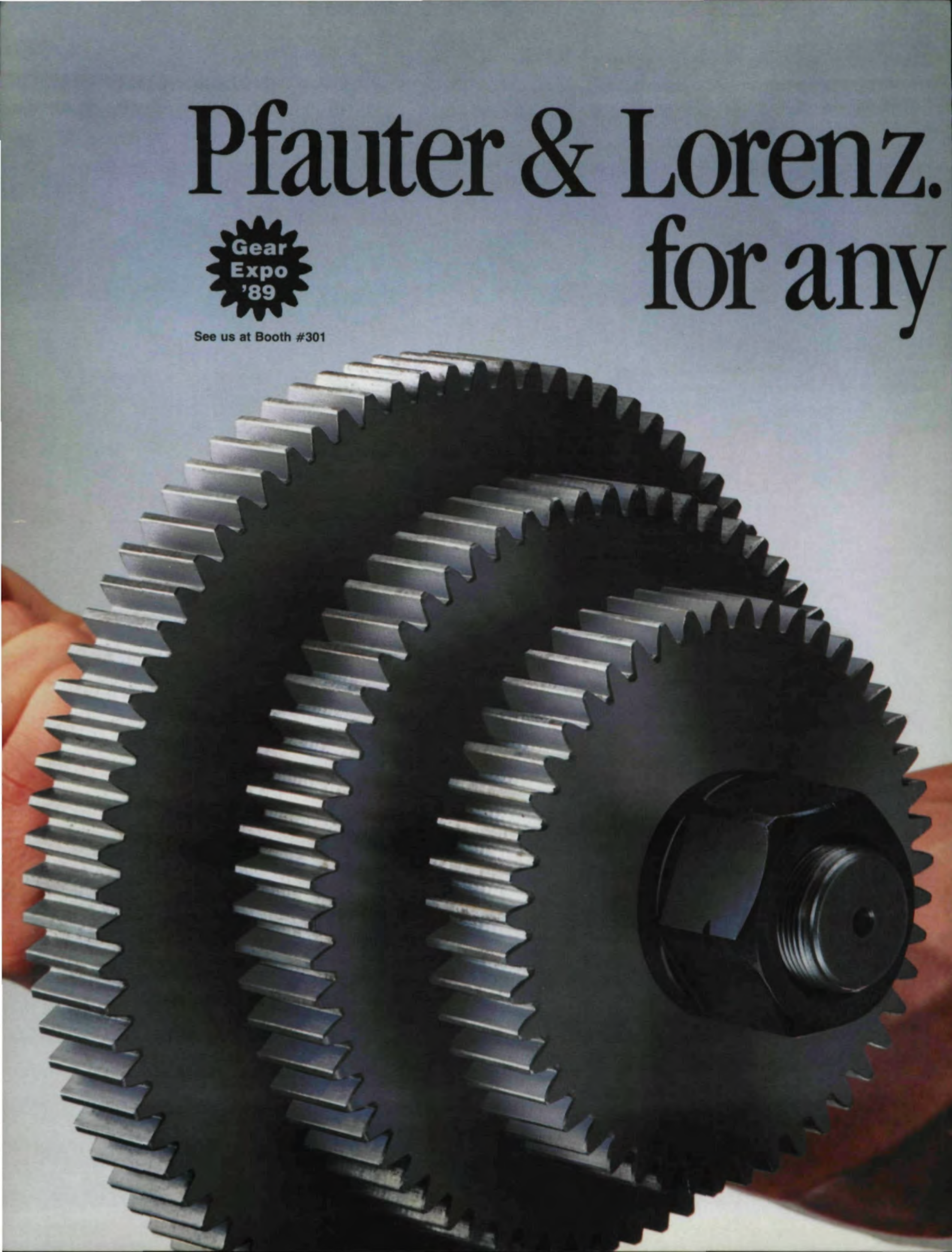
Pfauter & Lorenz.
for any
Gear
Expo
'89
See us at Booth #301

Powerful flexibility size job.

Pfauter CNC hobbers and Lorenz CNC shapers are used in more gear manufacturing applications than any other CNC machines. Why? Because of their complete flexibility to handle just about any lot size economically.

- Latest generation CNC controls make program preparation and execution an easy task for a single operator.
- Loading/unloading systems are designed to minimize non-productive time.
- Expandable storage capacity substantially increases unattended operation.
- Simple, quick-change tooling increases efficiency.

CAD/CAM designed and built by American Pfauter, these machines have become the reliable standards in aerospace, automotive, truck and tractor, and job shops of every size.

If you'd like to find out how Pfauter and Lorenz CNC technology can improve your productivity, contact American Pfauter, 925 Estes Ave., Elk Grove Village, IL 60007. Phone (312) 640-7500.

AMERICAN PFAUTER

Building American Productivity

CIRCLE A-1 ON READER REPLY CARD

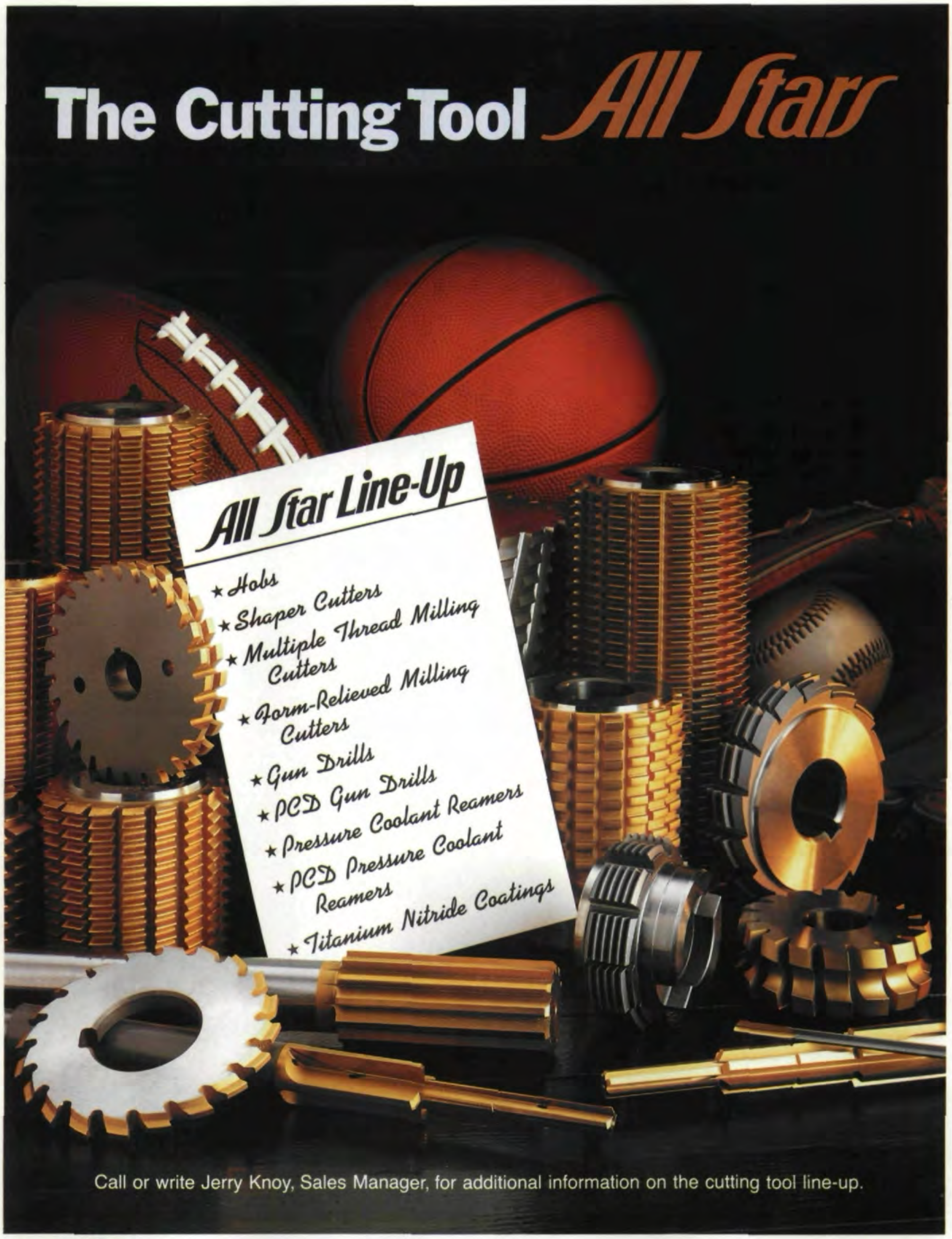
The Cutting Tool All Stars
All Star Line-Up
★ Hobs
★ Shaper Cutters
★ Multiple Thread Milling Cutters
★ Form-Relieved Milling Cutters
★ Gun Drills
★ PCD Gun Drills
★ Pressure Coolant Reamers
★ PCD Pressure Coolant Reamers
★ Titanium Nitride Coatings
Call or write Jerry Knoy, Sales Manager, for additional information on the cutting tool line-up.

RANDALL PUBLISHING
1401 Lunt Avenue
P.O. Box 1426
Elk Grove, IL 60007
(312) 437-6604

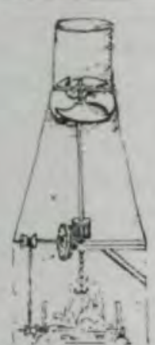

The Advanced Technology of Leonardo da Vinci 1452-1519

COVER

This sketch shows a heat driven roasting spit. The heat of the fire produces the energy to drive the airscrew, and the belt, pulleys, and a crown and lantern gear transmit motion down from the screw. In Leonardo's own words, "The roast will turn slow or fast, depending on whether the fire is small or strong." This sketch came to us courtesy of J. A. Broekhuisen of Rotterdam, The Netherlands, and Kip Newton of Reliance Electric, Greenville, SC.

GEAR TECHNOLOGY

The Journal of Gear Manufacturing

CONTENTS — PAGE NO.

FEATURES

DEPARTMENTS

July/August, 1989 — Vol. 6, No. 4

GEAR TECHNOLOGY, The Journal of Gear Manufacturing (ISSN 0743-6858) is published bimonthly by Randall Publishing Co., Inc., 1425 Lunt Avenue, P. O. Box 1426, Elk Grove Village, IL 60007. GEAR TECHNOLOGY, The Journal of Gear Manufacturing. Subscription rates are: $40.00 in the United States, $55.00 in Canada, $55.00 in all other foreign countries. Second-Class postage paid at Arlington Heights, IL and at additional mailing office.

Postmaster: Send address changes to GEAR TECHNOLOGY, The Journal of Gear Manufacturing, 1425 Lunt Avenue, P. O. Box 1426, Elk Grove Village, IL 60007.

MANUSCRIPTS: We are requesting technical papers with an educational emphasis for anyone having anything to do with the design, manufacture, testing or processing of gears. Subjects sought are solutions to specific problems, explanations of new technology, techniques, designs, processes, and alternative manufacturing methods. These can range from the "How to . . ." of gear cutting (BACK TO BASICS) to the most advanced technology. All manuscripts submitted will be carefully considered. However, the Publisher assumes no responsibility for the safety or return of manuscripts. Manuscripts must be accompanied by a self-addressed, self-stamped envelope, and be sent to GEAR TECHNOLOGY, The Journal of Gear Manufacturing, P.O. Box 1426, Elk Grove, IL 60009, (312) 437-6604.

Editorial

Publisher Michael Goldstein and Rick Norment, Executive Director, AGMA at Gear Expo '87.

Assorted thoughts while in a holding pattern over O'Hare . . .

I recently returned from England where I spent time checking out the overseas markets and attending a machinery auction. Buyers came to this auction from all over – Germany, Italy, Switzerland, India, Australia, America – and the prices were astonishing. Often buyers were paying in pounds sterling the same amount or more than they would have paid in U.S. dollars. In other words, they were paying, say, £10,000 for a machine that would have sold for $10,000 here. With every pound worth about $1.70 at today's exchange rates, that's a hefty 70% more than a comparable machine would cost here. Prices for consumer goods – food, clothing, automobiles, gasoline (£1.66 or $2.82 per U.S. gallon) – reflect the same price difference.

American products are very inexpensive on the world market today, and, judging from the prices at that auction in England, much of the industrialized world is not aware of the fact. I wonder how much of that ignorance is due to the fact that we simply have not done a very good job of selling ourselves overseas. Maybe we're not effectively informing the rest of the world that real estate is not the only bargain in the U.S. today. That 70% advantage is a powerful selling tool we should not neglect.

Other news from England: Long-time readers may remember that on my last trip to England, I spent a day at the races, driving some pretty impressive, powerful cars with my old friend Ian Exeter, part-owner of the company manufacturing the Lister Jaguar. This trip I didn't make it to the factory in Weatherhead, but I did get a preview of the newest high-tech toy for the super-rich – the Lister LeMans. This car is loosely based on the Jaguar XJ-S with a redesigned body and suspension and a 7-liter, V-12 engine capable of 496 BHP at 6200 rpm, with 500 lb/ft. of torque at 3250 rpm. Only the Calloway Twin Turbo Corvette, I believe, has better numbers, and that only with the torque. With a maximum speed of 200 mph, this supercar sells for a mere £121,000. (That's about $200,000 for those of you who keep your petty cash in U.S. currency.) Within weeks of the product announcement, deposits on a dozen of the cars had already been taken. Hard to believe there are folk around with that kind of loose change in their pockets. Next year, when I visit my son at school in England, I may get a chance to wrestle with this new breed of cat.

More mundane, but possibly more important matters: All reports I've received about the ASME 5th International Power and Transmission Gearing Conference have been excellent. This meeting, which is held only once every five years, draws gear engineering experts from all over the world. Some 125 papers on everything from gear design to manufacturing to belts and chains and couplings and clutches were presented. We were pleased to see a large number of our contributing authors there either as presenters or participants. The proceedings of the conference fill two fat books . . . Lots of important late night reading about the cutting edge of the industry between those orange covers . . . For those of you who missed it this time, it might be something to think about for 1994. A call to ASME for a list of the papers might be a worthwhile investment as well.

. . . AGMA's joint program with industry to get gear machinery into the hands of college engineering students is expanding. In June, Caterpillar is making available two Fellows gear shapers to qualified schools. Precision Gear of Twinsburg, OH, and Fairfield Manufacturing of Lafeyette, IN, have followed suit. Precision Gear has donated two Fellows shapers, one each to Ohio State and Central State University (Ohio). Fairfield has loaned

OSU tooling and has a program giving engineering students "hands on" experience at their Lafeyette facility. It's good to see some of you out there taking concrete steps to support our engineering schools and develop an interest in gearing among young engineers . . .

. . . AGMA's Gear Expo '89 is coming up faster than we think. If you haven't already made plans to attend, this is the time to do so. The Gear Expo is a good way to "take the pulse" of the industry. Gear Expo '89 will be 60% larger in terms of floor space than the 1987 show. A number of heavy machinery companies as well as other gear industry suppliers will be represented. The show is being held in conjunction with the AGMA Fall Technical Meeting, giving attendees the chance to both check out the new product lines and the new directions in gear engineering research. Pittsburgh will be the place to be in November to stay in touch with the gear business.

Michael Goldstein

Michael Goldstein, Editor/Publisher

ENGINEERING CONSTANTS

FORMULAS FOR DETERMINING GEAR DIMENSIONS BY METRIC PITCH

Module is the pitch diameter in millimeters divided by the number of teeth in the gear. Pitch diameter in millimetres is the Module multiplied by the number of teeth in the gear.

$$M = \frac{D'}{N} \text{ or } \frac{D}{N + 2}$$
$$D' = NM.$$
$$D = (N + 2)\ M.$$
$$N = \frac{D'}{M} \text{ or } \frac{D}{M} - 2$$
$$D'' = 2\ M.$$
$$t = M\ 1.5708.$$
$$f = \frac{M\ 1.5708}{10} = .157\ M.$$
$$M = \frac{25.4}{D.P.}$$
$$D.P. = \frac{25.4}{M}$$

The Module is equal to the part marked "S" in diagram, measured in millimeters and parts of millimeters.

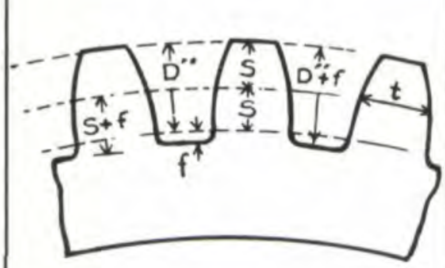

Pitches Commonly Used

Module	Corresponding English Diametral Pitch
½ mm.	50.800
¾	33.867
1	25.400
1.25	20.320
1.5	16.933
1.75	14.514
2	12.700
2.25	11.288
2.5	10.160
2.75	9.236
3	8.466
3.5	7.257
4	6.350
4.5	5.644
5	5.080
5.5	4.618
6	4.233
7	3.628
8	3.175
9	2.822
10	2.540
11	2.309
12	2.117
13	1.954
14	1.814
15	1.693
16	1.587

M&M Precision Systems . . .

the innovators in CNC gear inspection

Smart™ Probe package. LVDT probe and µprocessor-based convertor deliver high-speed data in µinches.

Operator Control Panel for part loading and machine set up.

Keyboard with "Mouse" for one-time entry of part print and tolerance data. "Mouse" permits use of CAD techniques.

Color graphics CRT with touch screen makes operation simple and fast.

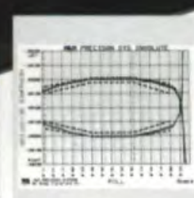

Graphics printer copies CRT.

Plotter delivers multi-color hard copy of graphics and test data.

CNC status monitor provides status and positional display of mechanical system and CNC control functions.

Our Model 3000 QC Gear Analyzer is a third generation CNC gear inspection system incorporating all of the comprehensive analytical tests and evaluation capabilities of previous M & M systems, such as our Model 2000, but with these added capabilities:

- Dramatically improved speed and accuracy through new mechanical system design and advanced CNC control technology.
- Computer hardware and applications software are modular to allow the user to buy only the required capability. This makes the 3000 QC adaptable to laboratory testing or production-line inspection.
- Integrated Statistical Process Control with local data base capability is an optional feature.
- Networking with MAPS compatibility is available.
- Robotic interfacing for totally automatic load/test/unload operation can be incorporated.

For more information or applications assistance, write or call: M & M Precision Systems, 300 Progress Rd., West Carrollton, OH 45449, 513/859-8273, TWX 810/450-2626, FAX 513/859-4452.

M&M PRECISION SYSTEMS

AN ACME-CLEVELAND COMPANY

CIRCLE A-6 ON READER REPLY CARD

TECHNICAL CALENDAR

JULY 12-14, 1989. ASM International Conference on Carburizing. Sheraton Hotel & Conference Center, Lakewood, CO. Tech conference for heat treaters, gear manufacturers, users of carburized metals. For more information, contact: ASM International, Metals Park, OH, 44073. (216) 338-5151 or fax (216) 338-4634.

SEPTEMBER 12-14, 1989. Short Course on Gear Noise. Ohio State University, Columbus, OH. This course will cover general noise measurement and analysis, causes of gear noise, noise reduction techniques, dynamic modeling, gear noise signal analysis, and modal analysis of gear boxes. For more information contact: OSU, Engineering Short Courses, 2070 Neil Avenue, Columbus, OH 43210-1275. Ph: (614) 292-8143. Fax: (614) 292-3163.

SEPTEMBER 12-20, 1989. European Machine Tool Show, Hannover, West Germany. Exhibits from 36 countries will show cutting and forming equipment, machine tools, CAD/CAM, robotics, etc. For more information, contact: Hannover Fairs, USA, Inc., 103 Carnegie Center, Princeton, NJ, 08540. (609) 987-1202.

NOVEMBER 6-8, 1989. AGMA Gear Expo '89, David Lawrence Convention Center, Pittsburgh, PA. Exhibition of gear machine tools, supplies, accessories and gear products. For more information, contact: Wendy Peidl, AGMA, 1500 King Street, Suite 201, Alexandria, VA, 22314. (703) 684-0211.

NOVEMBER 7-9, 1989, AGMA Fall Technical Meeting, Pittsburgh, PA. Seminars on a variety of gearing subjects held in conjunction with Gear Expo '89.

NOVEMBER 29 - DECEMBER 1. Fundamentals of Gear Design. Seminar, University of Wisconsin-Milwaukee. This course will cover basic design considerations in the development of a properly functioning gear system. It is planned with the designer, user and beginning gear technologist in mind. For more information, contact: Richard G. Albers, Center for Continuing Engineering Education, University of Wisconsin-Milwaukee, 929 North 6th Street, Milwaukee, WI, 53203. Ph: (414) 227-3125.

AGMA

GEAR EXPO '89

"THE CUTTING EDGE"

IN PITTSBURGH

DOWNTOWN

Framed by three picturesque rivers, Pittsburgh's Golden Triangle captures the essence of a cosmopolitan city without forfeiting its small town charm. Pittsburgh's Downtown area tastefully combines turn-of-the-century architectural masterpieces with uniquely styled structures to create a dazzling skyline. Within 10 square blocks, Pittsburgh offers first-class accommodations, diverse restaurants, fashionable shops, historic attractions and opulent entertainment facilities. Small parks, ideal for relaxing, are located throughout the heart of the city.

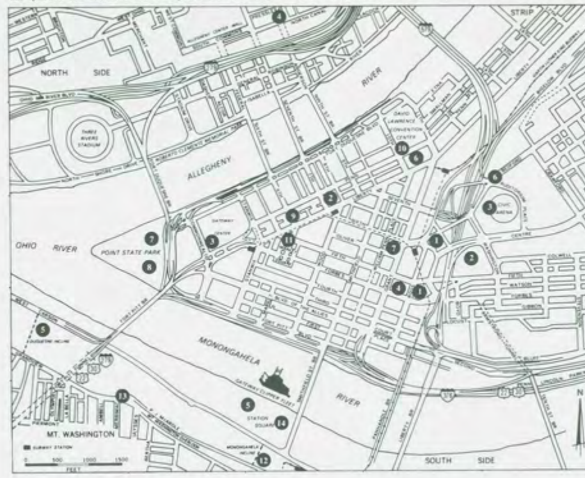

Points of Interest
1 Allegheny County Jail
2 Benedum Center for the Performing Arts
3 Civic Arena
4 Courthouse Galley/Forum
5 Duquesne Incline
6 Flag Plaza
7 Fort Pitt Blockhouse
8 Fort Pitt Museum
9 Heinz Hall
10 Lawrence Convention Center
11 Market Square
12 Monongahela Incline
13 Mt. Washington Overlook
14 Station Square

Accommodations
1 The Bigelow
2 Hyatt Pittsburgh
3 Pittsburgh Hilton and Towers
4 The Priory—A City Inn
5 Sheraton Hotel at Station Square
6 Vista International Hotel—Pittsburgh
7 Westin William Penn

AGMA's Gear Expo '89, "The Cutting Edge," opens at the David Lawrence Convention Center in Pittsburgh, PA, on Nov. 6 and runs through Nov. 8. This year's show is "the largest trade show ever conceived specifically for the gear industry," according to Rick Norment, AGMA's executive director. The show is 60% larger in terms of floor space than the 1987 show, and over 90% of the booths have been sold.

Gear Expo '89 seeks to offer gear manufacturers and suppliers to the gear industry a specialized forum where they can display their products. The world's major producers, suppliers, and heavy machinery manufacturers will be exhibiting, giving visitors the opportunity to make comparisons of products right at the show.

Among the products and services on display are grinders, hobbers, cutting tools, shapers, milling machines, testing equipment, filtration, lubricants, broaching, and heat treating.

The David Lawrence Convention Center is near the banks of the Allegheny River in the Golden Triangle section of downtown Pittsburgh. It is near major hotels, restaurants, and cultural attractions.

Show hours are 9:00 a.m. to 6:00 p.m. on Monday and Tuesday, and 9:00 a.m. to 4:00 p.m. on Wednesday.

In conjunction with the show and also at the Lawrence Convention Center, is the AGMA Fall Technical Conference. The conference will be held Nov. 7-9 and will feature papers on a variety of gearing subjects including, worm gears, gear dynamics, vibration analysis, lubrication, and gear geometry.

David Lawrence Convention Center

On The Interference of Internal Gearing

Dr. David D. Yu MPC Products Corp.

Skokie, IL

AUTHOR:

DR. DAVID YU *is a gearing specialist for MPC Products Corporation. Since 1982 he has been an Honorary Fellow of the University of Wisconsin at Madison. In the academic arena, he has served as the Deputy Head of the Mechanical Engineering Department and as Professor of Machine Design at Overseas Chinese University. Professor Yu is the author of numerous articles on gearing. He is a member of ASME Gear Research Institute.*

Introduction

Since size and efficiency are increasingly important considerations in modern machinery, the trend in gear design is to use planetary gearing instead of worm gearing and multi-stage gear boxes. Internal gearing is an important part of most of planetary gear assemblies. In external gearing, if the gears are standard (of no-modified addenda), interference rarely happens. But in an internal gearing, especially in some new types of planetary gears, such as the KHV planetary, the Y planetary, etc.,[1] various types of interference may occur. Therefore, avoiding interference is of significance for the design of internal gearing.

There are two categories of interference: cutting interference and meshing interference. The former is certainly related to the dimensions of the cutter. The latter is calculated through the dimensions of the meshing gears, which also bear relation to the cutter. Therefore, it is suggested that in calculating the geometrical dimensions and interferences of an internal gearing, the method of gear tooth generation and the parameters of the cutter to be used should be taken into account. However, this point of view has been neglected in most handbooks, textbooks and papers. For example, only one kind of interference is introduced and is based on the assumption that the gears are cut by a hob or a rack type cutter;[2] the formulae to determine the proportion of an internal gear tooth are borrowed from those for an external gear tooth;[3] and some standards, such as AGMA's, have not covered the internal gearing. Most internal and some external gears are cut by gear shaper cutters, not by hobs. The dimensions of a gear tooth cut by a shaper cutter are different from those cut by a hob. For designing an internal gearing, if we use the method based on hobbing and the formulae converted from those for external gearing, the data obtained seem to be correct, but practically, interferences may still exist, and sometimes the internal gear teeth cannot even be generated. Errors cannot be checked out because those formulae have no relation to the parameters of the cutter. Hence, for providing a correct calculation for geometrical dimensions and interferences, the methods of gear tooth generation and the parameters of the cutter should be discussed.

Methods for Gear Tooth Generation

Internal gears can be made by gear shaping, internal broaching, stamping, milling, etc. Some internal gears with large diameters can also be made by hobbing.[4] External gears can be made by hobbing, gear shaping, milling, rolling, etc. The most common method for generating internal gears is gear shaping, and for external gears is hobbing or gear shaping. In this article only these two methods will be discussed. For simplicity, "pinion" and "gear" are used for external gears and internal gears, respectively. The first thing that should be determined for designing an internal gearing is the method of generating gear teeth. There are two methods – shape-hobbed, wherein the gear is shaped and the pinion is hobbed, and double-shaped, where both the pinion and the gear are shaped.

Fig. 1 is the final position of cutting a pinion by a hob. M-M is the middle line on the hob. The root radius of the pinion cut by the hob is determined by this position; i.e.,

$$R_{f1} = 0.5N_1/P - a_h + X_1/P \quad (1)$$

where: R_{f1} – root radius of the pinion
N_1 – number of teeth of the pinion
P – diametral pitch of both the pinion and the hob
X_1 – addendum modification coefficient of the pinion
a_h – addendum of the hob.

Usually, $a_h = a + c$, where a is the standard addendum and c is the standard clearance.

The involute tooth profile is not an entire involute curve. It is composed of three different curves. The tip circle and the root circle are circular arcs. The active profile is an involute of a circle, which ends at the point K_1, where the tip of the hob intersects the line of contact pT. On the pinion from K_1 to the root, a curve is formed by the locus of the tip of the hob and is a modified involute of a circle (hidden line in Fig. 1). The pressure angle at the circle with radius $O_1 K_1$ is ϕ_{g1}, and

$$\text{TAN } \phi_{g1} = \text{TAN } \phi_o - 4(a_h P - X_1)/(N_1 \text{ SIN } 2 \phi_o) \quad (2)$$

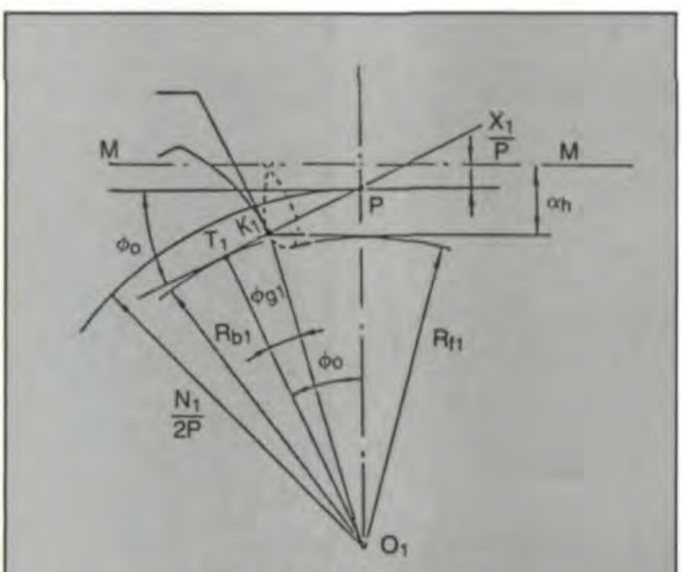

Fig. 1–Pinion Cut by Hob.

where ϕ_o is the standard pressure angle.

If the tip of the hob is rounded with a radius R_t, and $c > R_t (1 - \text{SIN } \phi_o)$, Equation 2 can still be used for calculating meshing interference.

Fig. 2 is the final position of cutting a pinion by a shaper cutter. The operating pressure angle between the cutter and the pinion at this position is ϕ_{1c}, and its involute function is

$$\text{INV } \phi_{1c} = 2 (X_1 + X_c) \text{ TAN } \phi_o/(N_1 + N_c) + \text{INV } \phi_o \quad (3)$$

where: N_c – number of teeth of the cutter
X_c – addendum modification coefficient of the cutter.

The center distance between the cutter center and the pinion center at this position is

$$C_{1c} = 0.5 (N_1 + N_c) \text{ COS } \phi_o/(P \text{ COS } \phi_{1c}) \quad (4)$$

The root radius of the pinion cut by the shaper cutter is determined by this final cutting position and the parameters of the cutter, or

$$R_{f1} = C_{1c} - R_{ac} \quad (5)$$

where R_{ac} is the radius of tip circle of the cutter.

The locus of the tip point K_1 on the cutter forms an epitrochoid on the fillet or the flank of the pinion (hidden line in Fig. 2). The pressure angle at the circle with radius $O_1 K_1$ is ϕ_{g1} and

$$\text{TAN } \phi_{g1} = (N_1 + N_c) \text{ TAN } \phi_{1c}/N_1 - N_c \text{ TAN } \phi_{ac}/N_1 \quad (6)$$

where ϕ_{ac} is the pressure angle at the tip circle of the cutter.

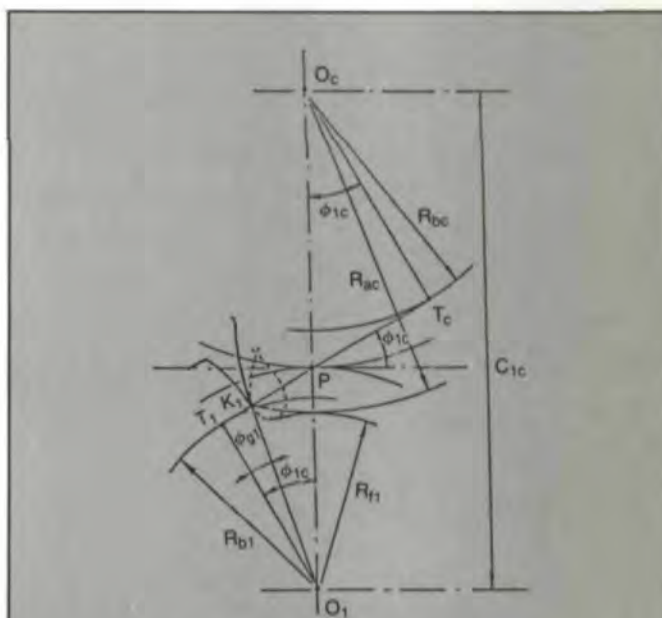

Fig. 2–Pinion Cut by Shaper Cutter.

Fig. 3 is the final position of cutting an internal gear by a shaper cutter. The operating pressure angle between the cutter and the gear at this position is ϕ_{2c}, and its involute function is

$$\text{INV } \phi_{2c} = 2\,(X_2 - X_c)\text{ TAN } \phi_o/(N_2 - N_c) + \text{INV } \phi_o \quad (7)$$

where: X_2 – addendum modification coefficient of the gear
N_2 – number of teeth of the gear.

The center distance between the gear center and the cutter center (O_2 and O_c) is

$$C_{2c} = 0.5\,(N_2 - N_c)\text{ COS } \phi_o/(\text{P COS } \phi_{2c}) \quad (8)$$

The root radius of the internal gear cut by the shaper cutter is determined by this position and the parameters of the cutter, or

$$R_{f2} = C_{2c} + R_{ac} \quad (9)$$

The locus of the tip point K_2 on the cutter forms a hypotrochoid on the flank or the fillet of the gear (hidden line in Fig. 3). The pressure angle at the circle with radius O_2K_2 is ϕ_{g2}, and

$$\text{TAN } \phi_{g2} = N_c \text{ TAN } \phi_{ac}/N_2 + (N_2 - N_c)\text{ TAN } \phi_{2c}/N_2 \quad (10)$$

From this, it is clear that the root radius of the gear, the root radius of the pinion and the tooth form are completely determined by the method of generating and the parameters of the cutter. The curve on the fillet portion of a tooth is a non-involute curve, such as hypotrochoid or modified involute or epitrochoid, and is called the transitional curve in this article.

Meshing Interference of Internal Gearing

An internal gearing has a much higher chance of interference than an external gearing. There are various meshing interferences, such as transitional interference, axial interference, radial interference, tip interference, inadequate clearance, etc., which will result in the failure of assembling or running or non-involute contact. During cutting, all the above interferences, except inadequate clearance, may occur too. Cutting interferences will result in undercut, trimming, etc.

Transitional Interference. If the tip of a gear falls into the region of the transitional curve on its mating gear, this pair of gears can not be assembled or there will be non-involute contact. Hence, it can not work, or the law of conjugation can not be satisfied. In many books (See Refs. 2, 5, 6, 7, 8), the point where the contact line is tangent to the base circle is taken as the end point of involute on the tooth. Therefore, interference can happen only "below the base circle". The calculation is simple, since there is no relation with the method of generation and the parameters of the cutters. However, it is incorrect because the ending point of the involute on the tooth is determined by the parameters of the cutter to be used, and usually this point is outside the base circle.

Fig. 4 shows an internal gearing during meshing. The center line is $O_1\,O_2$ and C is the center distance. $T_1\,T_2$ is the common tangent to the two base circles, R_{b1} and R_{b2}. The two tip circles R_{a1} and R_{a2} intersect $T_1\,T_2$ at B_2 and B_1, respectively. $B_1\,B_2$ is the interval of contact, and B_1 and B_2 are the beginning or ending point of contact. The pressure angle at the circle with radius $O_1\,B_1$ on the pinion is ϕ_{b1}, and the pressure angle at the circle with radius $O_2\,B_2$ on the gear is ϕ_{b2}. The operating pressure angle is ϕ, and ϕ_{a1} and ϕ_{a2} are the pressure angles at the two tip circles. Then

$$\text{TAN } \phi_{b1} = N_2 \text{ TAN } \phi_{a2}/N_1 - (N_2 - N_1)\text{ TAN } \phi/N_1 \quad (11)$$

$$\text{TAN } \phi_{b2} = N_1 \text{ TAN } \phi_{a1}/N_2 + (N_2 - N_1)\text{ TAN } \phi\,/N_2 \quad (12)$$

For avoiding the tip on the gear tooth interfering with the transitional curve on the pinion tooth, ϕ_{b1} should be larger than ϕ_{g1}, or

$$\text{TAN } \phi_{b1} > \text{TAN } \phi_{g1} \quad (13)$$

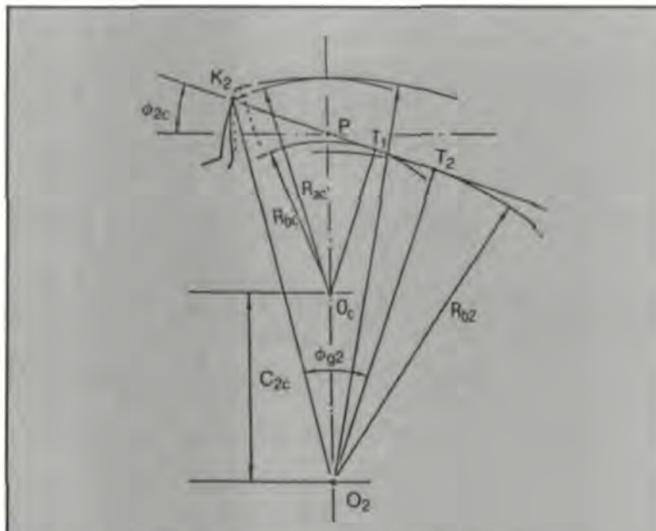

Fig. 3 – Internal Gear Cut by Shaper Cutter.

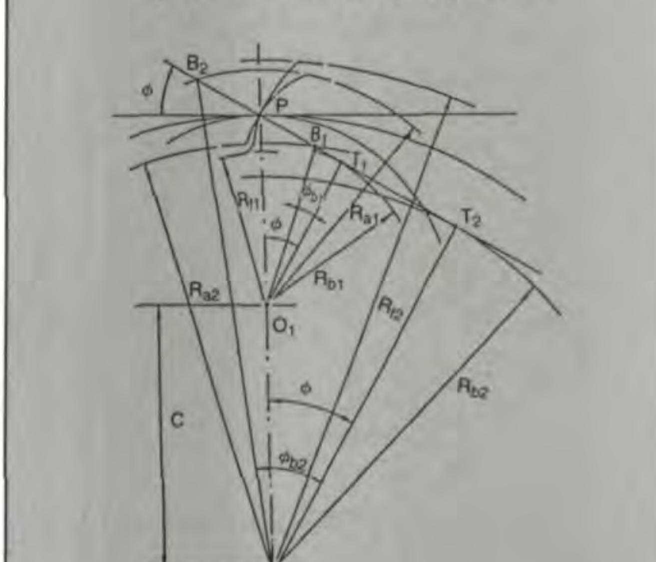

Fig. 4 – A Pair of Internal Gearing.

For shape-hobbed gearing and for double-shaped gearing, Eqs. 2 and 6, respectively, are used to calculate TAN ϕ_{g1}.

To avoid the tip of the pinion tooth interfering with the transitional curve on the gear, ϕ_{b2} should be smaller than ϕ_{g2}, or

$$\text{TAN } \phi_{b2} < \text{TAN } \phi_{g2} \tag{14}$$

Tip Interference. As shown in Fig. 5, when the difference in numbers of teeth $N_2 - N_1$ is small, the tip of the pinion may contact the tip of the gear at some place opposite to the pitch point. The following relationship will avoid tip interference:

$$R_{a2} + C > R_{a1} \tag{15}$$

Axial Interference. When the tooth difference $N_2 - N_1$ becomes small, after the involute meshing of a pair of teeth, the pinion tooth might contact the gear tooth again, which is called lap over, as shown in Fig. 6. Obviously, in such a case, the pinion can not be axially mounted into the gear. Therefore, this condition is called axial interference. For avoiding axial interference, the minimum tooth difference has been restricted to 10 or 12 for 20° pressure angle full depth teeth,[5, 9-11] without detail explanation and calculation formulae. But in some types of planetary gearing, for example, KHV planetary, the tooth difference is less than 6. In order to obtain a large speed ratio with a compact size and a high efficiency, use of the smallest tooth difference; i.e., $N_2 - N_1 = 1$ for the KHV planetary has been suggested.[12] This

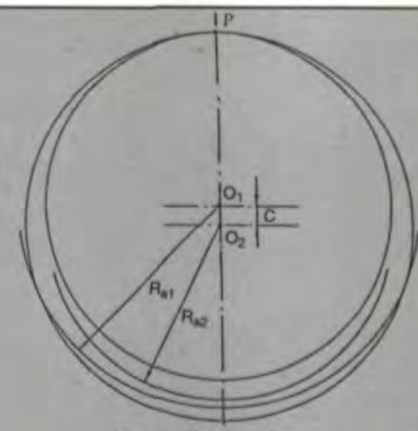

Fig. 5 – Tip Interference.

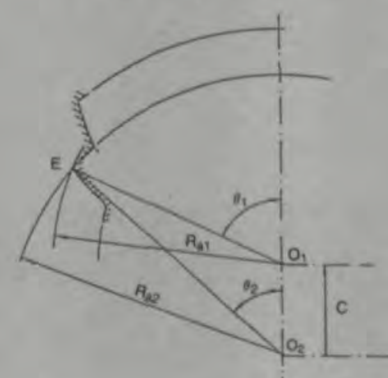

Fig. 6 – Axial Interference.

might be considered impossible according to the restriction in the above references, however, the KHV gear boxes with $N_2 - N_1 = 1$ have been successfully tested, not only working smoothly without any interference, but also reaching a high efficiency of 92% when speed ratio is as high as 120.

The place where the two tip circles intersect (point E in Fig. 6) is most vulnerable to axial interference. The condition for avoiding axial interference is calculated based on this point and is expressed as follows:

$$N_1\,(\theta_1 + \text{INV}\,\phi_{a1}) + (N_2 - N_1)\,\text{INV}\,\phi > N_2\,(\theta_2 + \text{INV}\,\phi_{a2}) \qquad (16)$$

where:
$$\theta_1 = \text{ARC COS}\,[(R_{a2}^2 - R_{a1}^2 - C^2)/(2R_{a1}\,C)] \qquad (17)$$
$$\theta_2 = \text{ARC COS}\,[(R_{a2}^2 - R_{a1}^2 + C^2)/(2R_{a2}\,C)] \qquad (18)$$

Radial Interference. If the tooth difference is small, radial interference may occur and the pinion cannot be radially mounted into the gear. Suppose in Fig. 7, after contact at point p, the pinion rotates an angle of β_1, and the gear rotates an angle of $\beta_2 = \beta_1 N_1/N_2$. If at this position L_2 is greater than L_1, there will be no interference along the $O_1 O_2$, or the radial direction. We can obtain through Fig. 7,

$$L_1 = R_{a1}\,\text{SIN}\,[\beta_1 - (\text{INV}\,\phi_{a1} - \text{INV}\,\phi)] \qquad (19)$$

$$L_2 = R_{a2}\,\text{SIN}\,[\beta_1 N_1/N_2 + (\text{INV}\,\phi - \text{INV}\,\phi_{a2})] \qquad (20)$$

and
$$F(\beta_1) = L_2 - L_1 > 0 \qquad (21)$$

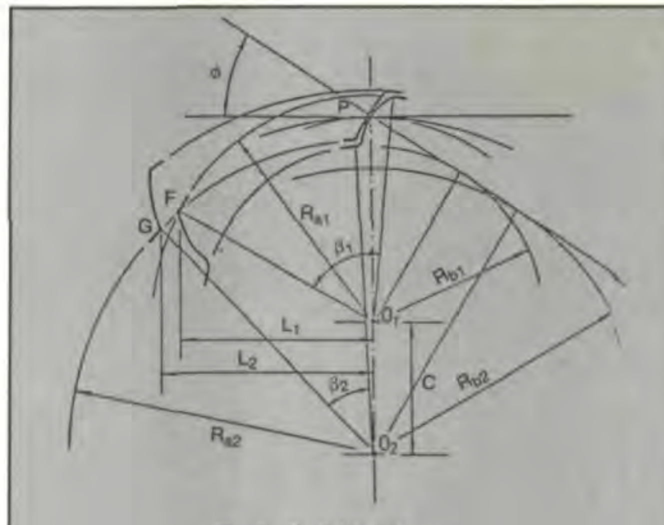

Fig. 7 – Radial Interference.

But this is for only one position of no interference. To avoid radial interference, all other positions should also satisfy Equation 21, including the minimum value of $F(\beta_1)$. Therefore, through Equation 21 and the differential of $F(\beta_1)$ equal to zero, we can eliminate β_1 and obtain the condition for avoiding radial interference as follows:

$$N_1\,\{\text{ARC SIN}\,\sqrt{[1-(\text{COS}\,\phi_{a1}/\text{COS}\,\phi_{a2})^2]/[1-(N_1/N_2)^2]} + \text{INV}\,\phi_{a1} - \text{INV}\,\phi\} >$$

FAST.

The CNC controlled HNC-35 Worm and Thread Grinder

Klingelnberg introduces the fastest . . . most accurate complex worm and thread grinder available . . . anywhere in the world! The CNC controlled HNC-35 stores data for up to 960 complex shapes, reducing set-up to 10-15 minutes . . . a fraction of the time required with mechanically controlled grinders.

The HNC-35 is versatile too. It performs creep-feed grinding from the solid, eliminating the need for preliminary milling of worms, threads and rotors. It's two machines in one . . . with the high degree of accuracy you'd expect from Klingelnberg.

See us at:

EMO — Hannover	AGMA — Pittsburgh
Sept. 12-20th	Nov. 6-8th
Hall 3, Booth B-005	Booth #101

KLINGELNBERG

The HNC-35 is available with a mechanical dresser or an optional CNC dresser, for special forms and flanks. Whether you produce small quantities or long production runs, the FAST set-up . . . FAST cycling . . . HNC-35 will improve your worm and thread productivity.

For additional information and a copy of our catalog, contact: Klingelnberg Corporation, 15200 Foltz Industrial Parkway, Cleveland, OH 44136. Or, phone (216) 572-2100 for an extra FAST response.

$$N_2 \{ARC\ SIN \sqrt{[(COS\ \phi_{a2}/COS\ \phi_{a1})^2 - 1]/[(N_2/N_1)^2 - 1]} + INV\ \phi_{a2} - INV\ \phi\} \quad (22)$$

Inadequate Clearance. As shown in Fig. 4, the clearance between the tip of the pinion 1 and the root of the gear 2 is

$$C_{12} = R_{f2} - C - R_{a1} \quad (23)$$

The clearance between the tip of gear 2 and the root of the pinion 1 is

$$C_{21} = R_{a2} - C - R_{f1} \quad (24)$$

If $C_{12} < 0$ or $C_{21} < 0$, there will be interference. The value of clearance should be adequate. If it is too small, the lubricant stored in it will be insufficient. On the other hand, if it is too large, sometimes the contact ratio will be decreased.

Cutting Interference

Undercut. When the cutter extends into the base circle of the pinion being cut, there will be undercut. The conditions for avoiding undercut are as follows:

for hobbed pinion, in Equation 2, $\phi_{g1} > 0$

and for shaped pinion, in Equation 6, $\phi_{g1} > 0$

Transition Interference. The shaper cutter can be considered as a gear. The fillet portion on the cutter is a transitional curve as on a gear. The pressure angle at the circle, on which the ending point of the involute profile is located, is ϕ_{gc}. Similiarly in Equation 2, we can obtain

$$TAN\ \phi_{gc} = TAN\ \phi_o - 4\ (a_h\ P - X_c)\ /\ (N_c\ SIN\ 2\ \phi_o) \quad (25)$$

where: a_h – addendum of the rack form cutter or the grinding wheel for generating the shaper cutter

X_c – addendum modification coefficient of the shaper cutter.

When a gear or a pinion is cut by a shaper cutter, if the tip of the gear reaches the transitional curve portion of the cutter, the tip of the gear teeth will not be formed to an involute curve. In other words, the involute on the tip is trimmed off. The conditions for avoiding transitional interference during cutting are as follows:

for pinion, $(N_1 + N_c)\ TAN\ \phi_{1c}/N_c - N_1\ TAN\ \phi_{a1}/N_c > TAN\ \phi_{gc}$ (26)

for gear, $N_2\ TAN\ \phi_{a2}/N_c - (N_2 - N_c)\ TAN\ \phi_{2c}/N_c > TAN\ \phi_{gc}$ (27)

Radial Interference. When a shaper cutter is cutting an interal gear, the cutter has a radial movement or a radial feed. If there is radial interference, the tip of the gear tooth will be trimmed. Equation 22 can be used for checking the radial interference during cutting, except that the subsript "1" should be changed to "c", and "ϕ" should be changed to "ϕ_{2c}".

Slight trimming on the tip of the gear teeth may help the load distribution on the teeth and decrease the dynamic load. Large trimming will seriously affect the contact ratio and other meshing indices.

No Involute. The operating pressure angle during cutting an internal gear by a shaper cutter is ϕ_{2c} and is determined by Equation 7.

The teeth difference between the gear and the cutter $N_2 - N_c$ should be greater than a minimum value, for example, 18 as shown in Reference 13. But this may not be sufficient. As discussed above, attention should be paid not only to the number of teeth, but also to other parameters of the cutter. Otherwise, in some cases, the gear cannot cut into the involute tooth profile.

Example 1. An internal gear has the following parameters: pressure angle $\phi_o = 20°$, module m= 2 mm, number of teeth $N_2 = 77$, whole depth = 2.25 m, addendum modification coefficient $X_2 = 0$. It is a common gear with standard tooth form. A shaper cutter, which is also one in some standard, has the following data: $\phi_o = 20°$, m = 2mm, number of teeth $N_c = 50$, addendum modification coefficient $X_c = 0.577$, whole depth 2.25 m. If the gear is cut by the cutter, from Equation 7, then:

$$INV\ \phi_{2c} = 2(0 - 0.577)\ TAN\ 20°/(77 - 50) + 0.0149044 = -0.00652$$

or $\phi_{2c} < 0$.

Therefore, this gear cannot be cut by this cutter, another kind of interference during cutting. It is suggested that the operating angle during cutting ϕ_{2c} be greater than 7 to 10°.

Design by Maximum Dimension, Check by Minimum Dimension

The importance of the method of generating gear teeth and the parameters of the cutters is clear now. But each time the shaper cutter is sharpened, its outside diameter is decreased, and so is the addendum modification coefficent X_c. In other words, some important parameters of the cutter are changing. If using the parameters of a new cutter to design an internal pair of gears with no interference, there still might be interference if the gears are cut with a sharpened cutter. Therefore, the author suggests designing a gearing by the maximum dimensions of the cutter and checking the obtained data through the minimum dimensions. The maximum dimensions are the sizes of a new cutter or the measured sizes of a sharpened cutter to be used for this design. The minimum dimensions are defined as the minimum outside diameter and the minimum addendum modification coefficient of the cutter. The minimum sizes of the cutter are determined by strength and the correct tooth form. With such minimum sizes the cutter can still perform a normal cutting. If there is interference checked by the minimum dimensions, the cutter cannot be used to its minimum sizes, and the limited sizes should be specified, or another cutter should be chosen. Two more examples are given for further illustration.

Example 2. A pair of internal gearings has the following parameters: $P = 8\ 1/\text{in}$, $\phi_o = 20°$, $N_1 = 15$, $N_2 = 45$, $X_1 = 0.4425$, $X_2 = 1.328$, $C = 1.97''$.
The pinion is hobbed, and the gear is cut by a shaper cutter. The parameters of the new cutter are: $\phi_o = 20°$, $N_c = 24$, $X_c = 0.2564$, $R_{ac} = 1.6883$ in, addendum $a_c = 1.25/P$. The minimum sizes of the cutter are: $(R_{ac})_{min} = 1.6050$in, $(X_c)_{min} = -0.41$.

a). Design through the new cutter.

The root radii are determined by the cutters. Through Equations 1, 7-9, we can obtain: $R_{f1} = 0.8366''$, $R_{f2} = 3.1082''$.

The tip radii are preliminarily determined by contact ratio and clearances and are checked by transitional interferences. $R_{a1} = 1.1100''$, $R_{a2} = 2.8350''$, Contact ratio $m_t = 1.438$, $C_{12} = 0.0282'' = 0.226/P$, $C_{21} = 0.0284'' = 0.227/P$.
Whole depth $h_1 = R_{a1} - R_{f1} = 0.2743'' = 2.187/P$
$h_2 = R_{f2} - R_{a2} = 0.2732'' = 2.186/P$

TAN $\phi_{b1} = 0.1641953 >$ TAN $\phi_{g1} = 0.1326991$ (no interference)
TAN $\phi_{b2} = 0.5889354 <$ TAN $\phi_{g2} = 0.6178138$ (no interference)

b). Check by the minimum sizes.

The root radius is changed to $R'_{f2} = 3.0794''$. The clearance becomes $C'_{12} = R'_{f2} - C - R_{a1} = -0.0006''$ Since $C^1_{12} < 0$, there is interference. The cutter cannot be used to its minimum sizes.

c). Limited sizes.

Try $(R_{ac})_{min} = 1.6563''$ and $(X_c)_{min} = 0$.
Then $R'_{f2} = 3.0978''$ and $C'_{12} = 0.0178'' = 0.142\ /P$.

In Reference 9 the minimum clearance is 0.157/P. Practically, the minimum value of clearance has relation to velocity, lubricant, etc. The obtained clearance is small, therefore, the outside radius of the cutter should not be sharpened less than 1.6563".

The term of TAN $\phi'_{g2} = 0.611423$ is less than TAN $\phi_{g2} = 0.6178138$ (for the new cutter), but is still larger than TAN $\phi_{b2} = 0.5889354$. Therefore, there is no transitional interference.

Example 3. A pair of internal gearings have the parameters: $\phi_o = 20°$, $m = 3.5$mm, $N_1 = 27$, $N_2 = 75$, $X_1 = 0.26$, $X_2 = -0.255$, $C = 82$mm. Both pinion and gear are cut by the same shaper cutter with parameters: $\phi_o = 20°$, $m = 3.5$mm, $N_c = 28$, $a_c = 1.3$ m. The cutter is not a new one. The measured sizes are $R_{ac} = 54.33$mm and $X_c = 0.229$. The minimum sizes are provided from some standard, $(R_{ac})_{min} = 53$mm, and $(X_c)_{min} = -0.157$.

a). Design through measured dimensions

The root radii are determined by the parameters of the cutter; $R_{f1} = 43.515$mm, $R_{f2} = 134.737$mm.

The tip radius of the pinion is preliminarily determined by clearance $C_{12} > 0.3m = 1.05$mm, and the tip radius of the gear is determined by transitional interference TAN $\phi_{b1} >$ TAN ϕ_{g1}. Then

$R_{a1} = 51.5$ mm $R_{a2} = 127.5$mm
$C_{12} = 1.237$mm $= 0.35$m, $C_{21} = 1.985$mm $= 0.567$m
TAN $\phi_{b1} = 0.227724 >$ TAN $\phi_{g1} = 0.1912166$ (no interference)
TAN $\phi_{g2} = 0.413594 >$ TAN $\phi_{b2} = 0.3916624$ (no interference)

contact ratio: $m_t = 1.55$
whole depth: $h_1 = 7.985$mm $= 2.28$m.
$h_2 = 7.237$mm $= 2.07$m.

b). Check by minimum sizes
$R'_{f1} = 43.605$mm $R'_{f2} = 134.909$mm
$C'_{12} = 1.409$mm $= 0.403$m $C'_{21} = 1.895$mm $= 0.541$m

TAN $\phi'_{g1} = 0.1733648 <$ TAN $\phi_{g1} = 0.1912166$

TAN $\phi'_{g2} = 0.4373599 >$ TAN $\phi_{g2} = 0.4135940$

For transitional interferences and clearance C_{12}, the gears cut by the sharpened cutter with minimum sizes are safer than those cut by the cutter with the measured sizes. The clearance C'_{21} is less than C_{21}, but is still greater than 0.3m. Therefore, the cutter can be used from the measured sizes to its minimum sizes for cutting this pair of internal gears.

(continued on page 43)

A New Method of Designing Worm Gears

by Michel Octrue C.E.T.I.M. Senlis, France

AUTHOR:

DR. MICHEL OCTRUE *received his degree in engineering at the E.C.A.M. of Lyon (France), and his degree Thesis at the University of Besançon (France). He is with the Gear Department of the Centre Technique des Industries Mécaniques (CETIM), where he is a specialist in worm gear practice and design. Dr. Octrue is a member of the International Standards Organization (ISO), Technical Committee 60 (Gears), Working Groups WG-4 (Nomenclature) and WG-7 (Worm Gears). He has done extensive work on experimental development of gear programs for computers and is a member of the national standard committees of Association Française de Normalisation (AFNOR) and Union de Normalisation de la Mécanique (UNM) for mechanical transmissions and gears.*

Abstract:

The first part of this article describes the analytical design method developed by the author to evaluate the load capacity of worm gears.

The second part gives a short description of the experimental program and testing resources being used at CETIM to check the basic assumptions of the analytical method; and to determine on gears and test wheels the surface pressure endurance limits of materials that can be used for worm gears.

The end of the article compares the results yielded by direct application of the method and test results.

Introduction

The main form of deterioration observed in worm gears is generally surface damage to the flanks of the gear wheel teeth, comparable to the pitting and flaking found in treated cylindrical gears. It is, therefore, essential to determine the load capacity of these gears by evaluating the torque that can be transmitted, which depends on the surface pressure the materials used can withstand. For this purpose, we developed a design model that can be used to determine the torque that can be transmitted with allowance for the distribution of the pressures along the lines of contact. This model was then experimentally verified using the admissible pressures of the materials as determined by a disk-and-roller simulator. We then compared the results obtained to those yielded by endurance tests carried out on gears.

Presentation of the Design Method

The design method we present here is an analytical method;[3] in other words, the gear is designed with allowance for the meshing conditions at all points of contact and at all times. These meshing conditions depend on the relative positions of the teeth of the gear and the threads of the worm, on the geometry of the contact (curvatures) and on the stiffness of the meshing teeth.

By contrast with some other methods,[6-7] the distribution of contact pressure is not assumed to be uniform at each instant of meshing, but is determined after the transmitted load has been distributed along the instantaneous line of contact. The distribution of the load is determined on the basis of the stiffness of the teeth and the stiffness of contact at each point of contact.

This method was developed in two stages:

First stage: development of a design model making it possible to establish the instantaneous distribution of the transmitted pressure from the geometry of the teeth, the geometry of contact and the mechanical properties of the materials of which the gear and worm are made.

Second stage: determination of the map of pressures along the lines of meshing contact. Since the maximum pressure between the teeth in contact is limited by the admissible pressure of the material, this makes it possible to determine the maximum transmissible load.

First step of the calculation. We first calculate the instantaneous load distribution between the flanks of the worm threads and the flanks of the gear teeth, with allowance for the operating geometry and the materials used.

This geometry results from the contact between the worm threads, generated by grinding or milling (A, I, N, K and other profiles) and the gear teeth, produced by cutting. It is theoretically determined from the basic geometrical characteristics of the worm and gear by calculating, in order:

- the profile of the worm threads according to the cutting method used;
- the transverse path of contact for each rack line of the worm;
- the field of contact or skewed surface on which the lines of contact evolve;
- the lines of contact at each instant of meshing;

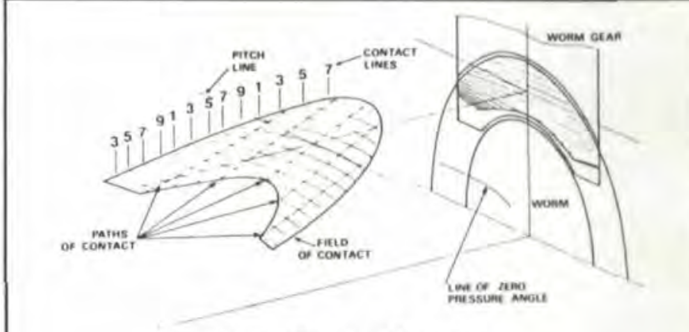

Fig. 1 – Operating Geometry.

- the equivalent radii of curvature and sliding velocities at each point of contact.

All of these calculations are based on the application of envelope theory and analytical geometry. They are made by breaking down the worm gear couple into a succession of elementary rack-and-pinion gears, having variable profiles determined in planes parallel to the midplane of the gear.

Fig. 1 shows the operating geometry of a worm gear having a 40:1 ratio. It shows:

- the transverse paths of contact in seven different rack lines;
- the field of contact with the lines of contact for five relative meshing positions (1, 3, 5, 7, 9);
- the line of zero pressure angle.

These various curves are represented in space and in projection in a plane perpendicular to the axis of the worm. Each point of the zone of contact is identified by two indices, i and j.

- i is the number of the line of contact;
- j is the number of the rack plane.

We define the stiffness of the gear tooth as $(R_R)ij$ and the stiffness of the worm thread as (R_vij) at each point of contact. To do this, we treat the toothing in each rack plane as a fixed-end beam of variable inertia (cf. Fig. 2).

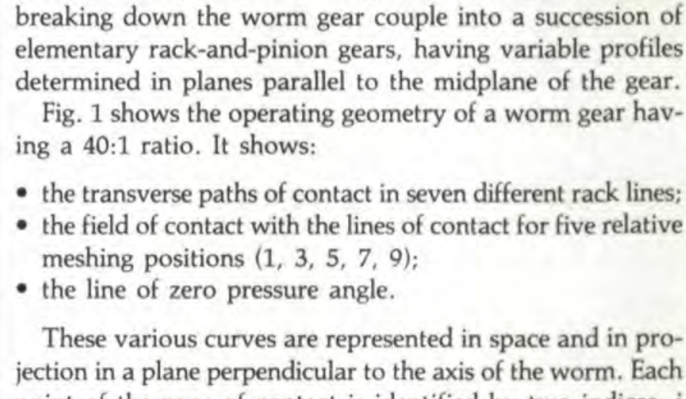

Fig. 2 – Calculation of stiffness.

The bending stiffness of these beams is determined by using Bresse's equations.[2] To determine the equivalent stiffness at the points of contact, we then apply the following two assumptions:

Assumption 1. During meshing, all the points of contact move uniformly, parallel to the operating reference plane of the worm because of the deformation of the teeth (Fig. 3).

Assumption 2. The initial pre-loading contact geometry is maintained during loading. This means that the displacements are sufficiently small and do not modify the initial field of contact.

In addition to the equivalent stiffness (RDeq)ij, the model takes the local contact stiffness (RC)ij into account.

In the zone of application of the load, the contact strains are broken down into deformation resulting from crushing of the teeth and deformation resulting from local compression of the part of the tooth under the contact.

The method used is the one developed and checked experimentally by Weber[8] for cylindrical gears. These deformations are not a linear function of the applied load, so an iterative method must be used to calculate the equivalent stiffness (Fig. 4).

At each point of contact we then have

(Req)ij = equivalent radius of curvature

(RDeq)ij = equivalent stiffness of teeth in contact

(RDeqm)ij = mean equivalent stiffness of the teeth in contact calculated along an elementary segment of the line of contact bounded by two successive rack planes.

(qz)ij = transmitted load density along an elementary segment of the line of contact

(RDeq)ij = takes the form

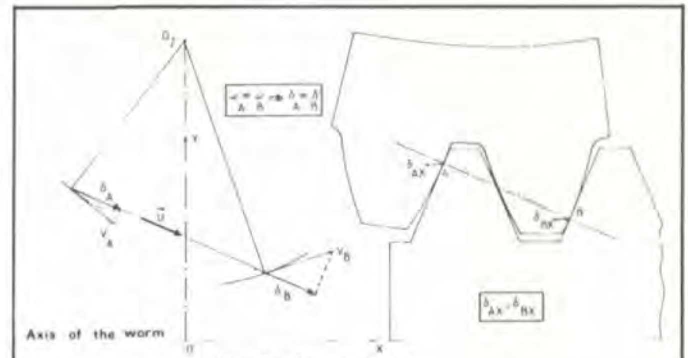

Fig. 3 – Assumption 1.

$$(RDeq)ij = \frac{1}{(R_R)ij} + \frac{1}{(R_v)ij} + \frac{1}{(RC)ij} \text{ parallel to the axis of the screw}$$

The total stiffness (RDG) of the gear parallel to the axis of the worm is given by:

$$RDG = \sum_{i_1\ j} (RDeq)ij$$

The total deformation at each point of contact, which we call δij, is the quotient of the mean load density divided by the mean equivalent stiffness. On the basis of Assumptions 1 and 2, we may state:

$$\delta ij = \frac{(qx)ij}{(RDeqm)ij} = \text{constant} = \delta$$

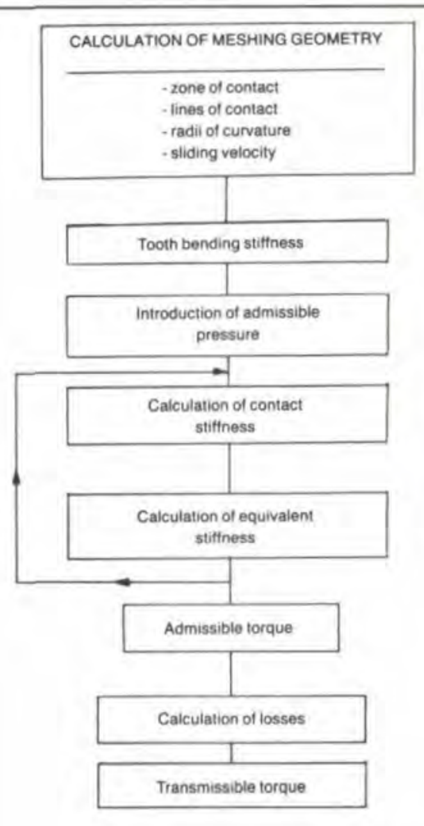

Fig. 4

DETERMINATION OF THE PRESSURES THE MATERIALS CAN WITHSTAND

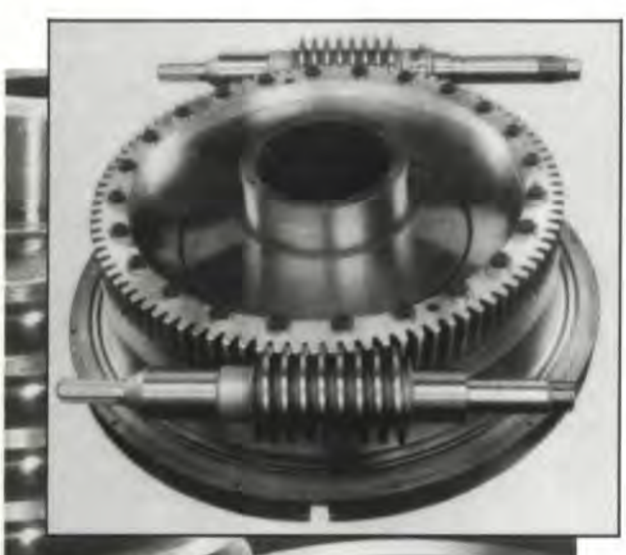

From the axial force transmitted to the worm and the total stiffness of the worm RDG calculated above, we obtain:

$$\delta = \frac{QX}{RDG} = \delta ij$$

From the mean equivalent stiffness, we determine the distribution of the transmitted load (qx)ij along the lines of contact:

$$(qx)ij = \delta.(RDeqm)ij$$

Second step of the calculation. From the load distribution, which is now known, it is possible to determine the contact pressure at each point of the meshing zone. The maximum pressure found must be less than the admissible pressure of the material σ_{Hlim}. This value is determined experimentally for each material.

Therefore, if we know the materials and the geometry used, it will be possible to reverse the calculation to determine the admissible pressure σ_{Hlim}, to determine the load distribution along the lines of contact and the admissible load on the teeth, and so finally to determine the admissible torque. For this, we use the following procedure. At each point, the contact pressure obtained by applying Hertz's theory (cylindrical contact) is given by

$$(P_M)ij = ZE \sqrt{\frac{QX}{RDG} \cdot \frac{(RDeqm)ij}{(Req)ij\ (X_N)ij}} = ZE \sqrt{\frac{QX}{RDG} \frac{1}{Kij}}$$

where:

$(X_N)ij$ = direction cosine of the normal to the plane of contact

Kij = curvature-rigidity factor $Kij = \left(\frac{Req.\ X_N}{RDeqm}\right)_{ij}$

ZE = elasticity factor such that

$$ZE = \frac{1}{\sqrt{\pi\left(\frac{1-\nu_1^2}{E_1} + \frac{1-\nu_2^2}{E_2}\right)}}$$

with $\left.\begin{array}{l}\nu_1,\ \nu_2 = \text{Poisson's ratio}\\ E_1,\ E_2 = \text{Young's moduli}\end{array}\right\}$ of materials involved

We must verify that

$$(P_M)ij \leqslant \sigma_{Hlim}$$

which allows us to write:

$$QX \leqslant \left(\frac{\sigma_{Hlim}}{ZE}\right)^2 \cdot RDG \cdot Kij$$

At the limit, the maximum load capacity is obtained for the minimum value of Kij = $(Kij)_{mini}$

then

$$QX_{max} = \left(\frac{\sigma_{Hlim}}{ZE}\right)^2 \underbrace{[RDG_P \cdot (Kij)_{minip}]}_{ZR}$$

ZR = pressure distribution factor of the gear.

NOTE: Index p refers to the relative position of the gear and worm. p is chosen so that product $RDG_P \cdot (Kij)_{miniP}$ is minimized, defining ZR. The admissible torque on the gear is then:

$$C = 5.10^{-4} \cdot d_{w2} \left(\frac{\nu_{Hlim}}{ZE}\right)^2 ZR \text{ in m.N}$$

with d_{w2} = pitch diameter of the gear wheel.

Calculation of losses. From the sliding velocity, taking into account the coefficient of friction variation, which is a function of sliding value, it is possible to calculate the power loss at each point of contact and so calculate the instantaneous efficiency of the gearing η.

The true torque that can be transmitted to the gear is then:

$$C_r = \eta.C$$

The calculation method described is, therefore, based on calculating the distribution of stiffness and the distribution of contact pressure during meshing (ZR factor). If the maximum pressure is limited to the admissible pressure of the material δ_{Hlim}, the admissible torque can be deduced and from it, by evaluating the losses in the gearing, the torque that can be transmitted.

The ZR factor is determined using the CADOR-ROUVIS software.

The diagram below shows the various steps of the calculations required for the application of the method described above.

Generally speaking, the load capacity of worm gears is limited by the performance of the material of the gear wheel.

The admissible pressure of this material is determined by evaluating its contact pressure endurance curve. This curve is determined experimentally on a disk roller simulator designed and built at CETIM. *(continued on page 40)*

Introducing the

COME UP TO SPEED WITH THE OERLIKON GEAR MANUFACTURING PROGRAM

OERLIKON CNC SPIROMATIC S20, S30, BEVEL GEAR GENERATORS—Cut either parallel or tapered depth teeth on one Oerlikon CNC Bevel Gear Cutting Machine.

OERLIKON CNC SPIROMATIC B20 BLADE GRINDER—Grind any type bevel gear cutting blade on one Oerlikon CNC Blade Grinder.

OERLIKON CNC SPIROMATIC X20 BEVEL GEAR GRINDER—Grind any bevel gear system with CBN on one Oerlikon CNC Gear Grinder.

OERLIKON CNC SPIROMATIC L20 BEVEL GEAR LAPPER—Full CNC control increases productivity and flexibility.

OERLIKON CNC-MAAG OPAL SPUR & HELICAL GEAR GRINDER—The MAAG tradition of quality built for tomorrow's productivity for spur and helical gearing.

The machines, that make the gears, that turn the wheels

Competition.

OERLIKON

GEAR MACHINES

Machine Tool Works
Oerlikon—Bührle Ltd.
Birchstrasse 155
8050 - Zurich, Switzerland
Phone 01/316 22 11
Telex 823 205 WOB CH
FAX 01/312 42 87

CIRCLE A-13 ON READER REPLY CARD

Into-Mesh Lubrication of Spur Gears Part 2

L. S. Akin Gear Consultant, Banning, CA and

D. P. Townsend NASA Lewis Research Center Cleveland, Ohio

AUTHORS:

DR. LEE S. AKIN *has been working in mechanical engineering since 1947, specializing principally in technologies related to rotating machinery. About half of this time has been spent in the gear industry and the other half in the aerospace industry, concentrating on mechanisms involving gears and bearings as well as friction, wear, and lubrication technologies.*

Since 1965, when he received his Ph.D. in mechanical engineering, he has been extensively involved in gear research especially related to the scoring phenomena of gear tooth failure. In 1971 he joined forces with Mr. Dennis Townsend of NASA Lewis Research Center, and together they have produced numerous papers on technologies related to gear scoring. Since 1986, Dr. Akin has been working as a gear consultant with his own company, Gearsearch Inc.

MR. D.P. TOWNSEND *is a gear consultant for NASA and numerous industrial companies. Townsend earned a BSME from the University of West Virginia. During his career at NASA he has authored over fifty papers in the gear and bearing research area. For the past several years, he has served in active committee roles for ASME. Presently he is a member of the ASME Design Engineering Executive Committee.*

Abstract:

An analysis was conducted for into-mesh oil jet lubrication with an arbitrary offset and inclination angle from the pitch point, for the case where the oil jet velocity is equal to or greater than pitch line velocity. Equations were developed for the minimum and the maximum oil jet impingement depth. The analysis also included the minimum oil jet velocity required to impinge on the gear or pinion and the optimum oil jet velocity required to obtain the best lubrication condition of maximum impingement depth and gear cooling. It was shown that the optimum oil jet velocity for best lubrication and cooling occurs when the oil jet velocity equals the gear pitch line velocity. When the oil jet velocity is slightly greater than the pitch line velocity, the loaded side of the driven gear and the unloaded side of the pinion receive the best lubrication and cooling with slightly less impingement depth. As the jet velocity becomes much greater than the pitch line velocity, the impingement depth is considerably reduced and may completely miss the pinion.

Introduction

In the lubrication and cooling of gear teeth a variety of oil jet lubrication schemes is sometimes used. A method commonly used is a low pressure, low velocity oil jet directed at the ingoing mesh of the gears, as was analyzed in Reference 1. Sometimes an oil jet is directed at the outgoing mesh at low pressures. It was shown in Reference 2 that the out-of-mesh lubrication method provides a minimal impingement depth and low cooling of the gears because of the short fling-off time and fling-off angle.[3] In References 4 and 5 it was shown that a radially directed oil jet near the out-of-mesh position with the right oil pressure was the method that provided the best impingement depth. Reference 6 showed this to give the best cooling. However, there are still many cases where into-mesh lubrication is used with low oil jet pressure, which does not provide the optimum oil jet penetration and cooling. It should also be noted that excessive into-mesh lubrication can cause high losses in efficiency from gear churning and trapping in the gear teeth.[7] In Reference 8 the case for into-mesh lubrication with oil jet velocity equal to or less than pitch line velocity was analyzed, and equations were developed for impingement depth for several jet velocities.

The objective of the work reported here was to develop the analytical methods for gear lubrication with the oil jet directed into mesh and with the oil jet velocity equal to or greater than the pitch line velocity. When the oil jet velocity is greater than the pitch line velocity for into-mesh lubrication, the impingement depth is determined by the trailing end of the jet after it has been cut off or chopped by the following tooth. The analysis is therefore somewhat different from Part I of this article[8] for the case where the oil jet velocity is less than the pitch line velocity. The oil jet location should be offset from the pitch point with an inclined angle to obtain optimum cooling of both gear and pinion for other than one-to-one gear ratios.

The analysis presented here assumes an arbitrary offset and inclination angle to obtain an optimum oil jet velocity for various gear ratios. Further analysis is needed to determine the optimum offset and inclination angle for various gear ratios.

Analysis

The high-speed cooling jet conditions discussed in this analysis are used only when a range of duty cycle conditions dictate a wide operating speed range with a constant oil jet velocity that must be suitable over the whole range of speeds. Starting with Fig. 1 the sequence of events for the pinion in the case where $V_j > \omega_p r \sec \beta_p$ is shown in Figs. 1 through 4. Here, instead of tracking the head of the jet stream as in Part I of this article,[8] the trailing end or "tail" of the stream will be tracked after it is chopped by the gear tooth.[1] This is shown at "A" in Fig. 3 to the final impingement at a depth "d_p" on the pinion tooth 2 as shown in Fig. 4. Initial impingement on the pinion starts as the pinion top land leading edge crosses the jet stream line with inclination angle set at β_p and offset S_p as shown in Fig. 1.

The position of the pinion at this time is θ_{p3}, defined (from Fig. 1) as:

$$\theta_{p3} = \cos^{-1}(r_s/r_o) - \text{inv}\,\varphi_{op} + \text{inv}\,\varphi \tag{1}$$

where:

$$\text{inv}\,\varphi_{op} = \tan\varphi_{op} - \varphi_{op} \text{ and}$$
$$\varphi_{op} = \cos^{-1}(r_b/r_o)$$

$$\text{inv}\,\varphi = \tan\varphi - \varphi$$

Generally the arbitrarily set offset "S" for the gear establishes the value of β_p from:

$$\beta_p = \tan^{-1}[S/(R_o^2 - R_s^2)^{1/2}] \tag{2}$$

Given β_p, then s_p can be calculated from

$$S_p = [(r_o^2 - r^2\cos^2\beta_p)^{1/2} + r\sin\beta_p]\sin\beta_p \tag{3}$$

so that:

$$r_s = r - S_p$$

The tail of this jet stream is finally chopped at "A" in Fig. 3 by the gear top land leading edge. The position of the gear at this time is θ_{g1} calculated:

$$\theta_{g1} = \cos^{-1}(R_s/R_o) - \text{inv}\,\varphi_{og} + \text{inv}\,\varphi \tag{4}$$

where:

$$\text{inv}\,\varphi_{og} = \tan\varphi_{og} - \varphi_{og} \text{ and}$$

$$\varphi_{og} = \cos^{-1}(R_b/R_o)$$

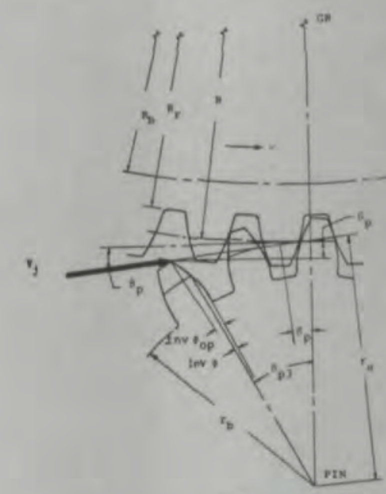
Figure 1.

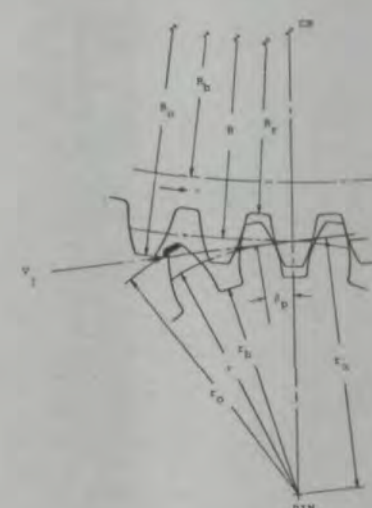
Figure 2.

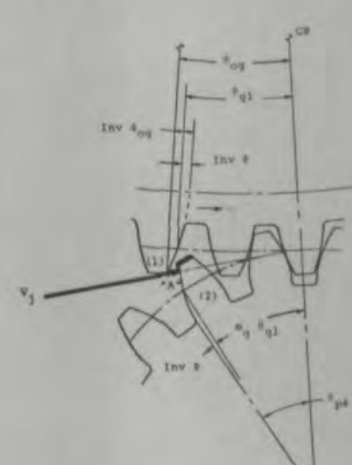
Figure 3.

Nomenclature

a	$1/P_d$ or $(1 \pm \Delta N/2)/P_d$ = addendum	t	time
b_p, b_g	pinion and gear backlash, respectively	t_f, t_ω	time of flight, rotation
B_p, B_g	total, pinion, gear backlash at $P_d = 1$	$V_p = V_g$	linear velocity of pinion and gear at pitch line
d_p, d_g	radial impingement depth	V_j, V_{jp}	oil jet velocity, general, pinion controlled
L_p, L_g	pinion, gear final impingement distance	x	distance from offset perpendicular to jet line intersection
L_{ig}	intermediate impingement distance		
m_g	$N_g/N_p = R/r = \omega_p/\omega$ = gear ratio	$V_j(\max)_p$	maximum velocity at which $d_p = 0$
N_p, N_g	number of teeth in pinion, gear	$V_j(\min)_p$	minimum velocity at which $d_p = 0$
ΔN	differential number of teeth	β	arbitrary oil jet inclination angle
P_d	diametral pitch	β_p	constrained inclination angle
r, R	pinion and gear pitch radii	β_{pp}	inclination angle for pitch point intersection
r_α, R_α	perpendicular distance from pinion, gear center to jet line	φ	pressure angle at pitch circles
		φ_{pi}, φ_{gi}	pinion and gear pressure angle at points specified at i
r_s, R_s	distance along line of centers to jet line origin		
r_x, R_x	distance along line of centers to jet line intersection at x	ω_p, ω_g	pinion gear and angular velocities
		inv φ	$\tan \varphi - \varphi$ = involute function at pitch point or operating pressure angle
r_o, R_o	pinion and gear outside circle diameter		
r_b, R_b	pinion and gear base radii	$V_j(\text{Opt}, U)_p$	upper limit jet velocity to impingement at pitch line (at upper end of plateau)
S, S_o, S_p	arbitrary jet nozzle offset to intersect O.D.'s offset for pinion only		

Then the position of the pinion at time equal to zero ($t = 0$) is calculated from:

$$\theta_{p4} = m_g\theta_{g1} + \text{inv}\,\varphi \tag{5}$$

which locates the pinion at the time of the flight of the *tail* of the jet stream when it is initiated. (See Fig. 3.) The jet tail continues to approach the trailing side of the pinion tooth profile until it reaches the position shown in Fig. 4, when it terminates at time $t = t_f$. The position of the pinion at this time is calculated from:

$$\theta_{p5} = \tan^{-1}\left(\frac{L_p \cos \beta_p}{r - L_p \sin \beta_p}\right) + \text{inv}\,\varphi_{p5} \tag{6}$$

where:

$$\text{inv}\,\varphi_{p5} = \tan \varphi_{p5} - \varphi_{p5}$$

$$\varphi_{p5} = \cos^{-1}\left(\frac{r_b}{[(r - L_p \sin \beta_p)^2 + (L_p \cos \beta_p)^2]^{1/2}}\right) \tag{7}$$

(See Fig. 4.)

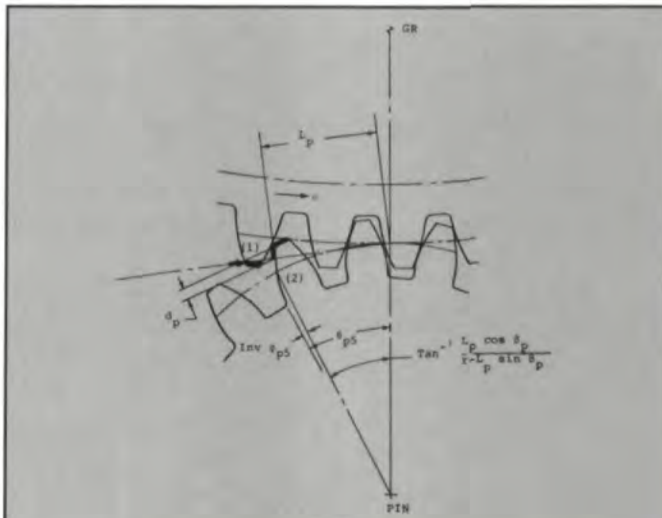

Figure 4.

TABLE 1. – EQUATIONS FOR OIL JET VELOCITY AND PINION IMPINGEMENT DEPTH FOR PITCH LINE AND HIGHER OIL JET VELOCITY

Relative velocity scale	Oil jet velocity	Pinion Impingement Depth
Critical high velocity to miss the pinion	$V_j(\max)_p = \frac{*[(R_o^2 - R_s^2)^{1/2} \sec \beta_p - (r_o^2 - r_s^2)^{1/2} \sec \beta_p]\,\omega_p}{\theta_{p6} - \theta_{op}}$ $V_j(\max)_p \to \infty$, when $s = s_o$ and $\beta_p = \beta_{pp}$	$d_p(\min, U) = 0^*$ $(m_g = 1)$ *when $m_g \geq m_g(\text{crit})$ and $0 \leq s < s_o$ and $0 \leq \beta_p < \beta_{pp}$
Higher than pitch line velocity up to where the jet starts to miss the pinion	$V_j = \frac{\omega_p[(R_o - R_s)^{1/2} \sec \beta_p - L_p]}{\theta_{p4} - \theta_{p5}}$ V = given (when $0 \leq d_p \leq a$ <u>only</u>)	d_p = given (usual design solution and $L_p = [(r_o - d_p)^2 - r^2 \cos^2 \beta_p]^{1/2} + r \sin \beta_p$ Iterate L_p from: $[(R_o^2 - R_s^2)^{1/2} \sec \beta_p - L_p]\,\omega_p = (\theta_{p2} - \theta_{p1})V_j$ $d_p = r_o - [(r - L_p \sin \beta_p)^2 + (L_p \cos \beta_p)^2]^{1/2}$
Slightly higher and pitch line-upper end of velocity plateau	$V_j(\text{opt}, U)_p = \frac{\omega_g(R_o^2 - R_s^2)^{1/2} \sec \beta_p}{\theta_{g1}}$ $V_j = \omega_p r \sec \beta_p = \omega_g R \sec \beta_p$	$d_p(\text{tail}) = a$, (trailing profile only) $d_p = a = (1 \pm \Delta N_p/2)/P_d$, (both profiles)

The *design* solution to the problem of pinion cooling when "d_p" is specified is to solve explicitly for the jet V_j based on the fact that $t_f = t_\omega$ as shown in Part I of this article. Thus, the required jet velocity is calculated from:

$$V_j = \frac{[(R_o^2 - R_s^2)^{1/2} \sec \beta_p - L_p]\omega_p}{\theta_{p4} - \theta_{p5}} \qquad (8)$$

where:

$$L_p = [(r_o - d_p)^2 - r^2 \cos^2 \beta_p]^{1/2} + r \sin \beta_p \qquad (9)$$

The *analysis* solution to the problem when V_j is specified $[V_j(\text{Opt, U})_p < V_j < \infty]$ so that the resulting impingement depth d_p, can be calculated implicitly by solving iteratively for "L_p" from:

$$\omega_p[(R_o^2 - R_s^2)^{1/2} \sec \beta_p - L_p] = (\theta_{p4} - \theta_{p5})V_j \quad \text{then} \qquad (10)$$

$$d_p = r_o - [(r - L_p \sin \beta_p)^2 + (L_p \cos \beta_p)^2]^{1/2} \qquad (11)$$

(See Fig. 1.)

Moving up along the velocity scale of Table 1 from $\omega_p r \sec \beta_p = V_j$, it can be shown that the upper limit $V_j(\text{Opt, U})$ for the "constant impingement depth range" where $d_p = a$, can be calculated for the pinion from:

$$V_j(\text{Opt, U})_p = \omega_g(R_o^2 - R_s^2)^{1/2} \sec \beta_p / \theta_{g1} \qquad (12)$$

Thus, if the jet velocity V_j is between the lower limit $V_j(\text{Opt, L})_p < V_j < V_j(\text{Opt, U})_p$, then the impingement depth will be $d_p = a = 1/P_d$ on at least one side of the tooth profile. If $V_j = \omega_p r \sec \beta_p$ exactly, then *d_p = a on both sides of the tooth profile.* Increasing the jet velocity above $V_j(\text{Opt, U})_p$ reduces the impingement depth d_p until at $V_j(\max)_p$ the tail of the jet chopped by the gear tooth is moving so fast as to be just missed by the pinion top land leading edge "A" in Fig. 6 when $m_g > m_g(\text{crit})$. The upper limit critical gear ratio, as a function of N_p and assuming $V_j(\max)_p = \infty$, may be calculated from:

$$m_g(\text{crit}) = \frac{\cos^{-1}\dfrac{N_p}{N_p + 2} - \text{inv}\left(\cos^{-1}\dfrac{N_p \cos\varphi}{N_p + 2}\right) + \text{inv}\varphi + \pi/N_p - 2B_p/N_p}{\cos^{-1}\left(\dfrac{m_g(\text{crit})N_p + 2P_dS}{m_g(\text{crit}) + 2}\right) - \text{inv}\cos^{-1}\left(\dfrac{N_p \cos\varphi}{N_p + 2/m_g(\text{crit})}\right) + \text{inv}\varphi} \qquad (13)$$

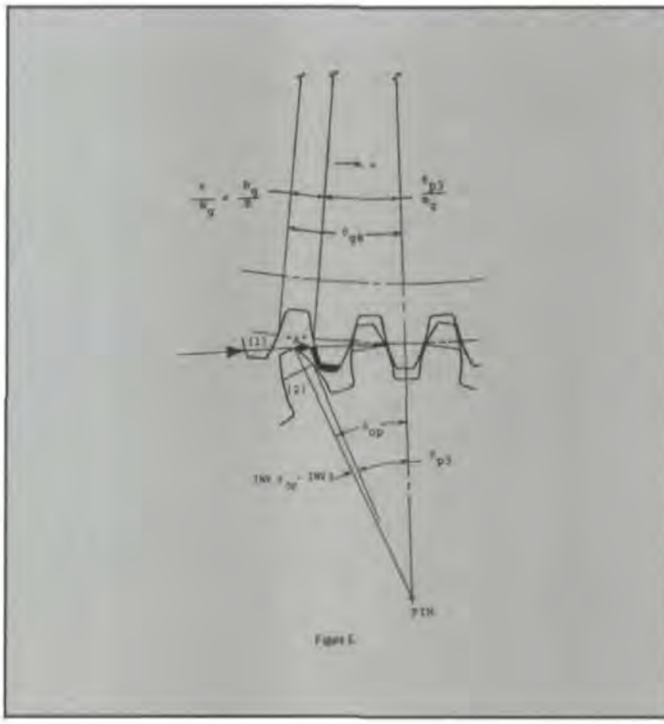

where:

$$N_p' = [N_p \cos^2 \beta_p - \{(N_p + 2)^2 - N_p^2 \cos^2 \beta_p\}^{1/2} \sin \beta_p] \tag{14}$$

and

$$\beta_p = \tan^{-1} \{S\, P_d / [m_g(\text{crit}) N_p (1 - P_d S)^2 - (P_d S)^2]^{1/2}\} \tag{15}$$

and

$$P_d S = \frac{(S/S_o)[m_g(\text{crit}) - 1]}{[m_g(\text{crit}) + 1]} \tag{16}$$

when $S = S_o$ and $\beta = \beta_{pp}$, $V_j(\max)_p < \infty$, the $m_g(\text{crit})$ ceases to exist.

When the maximum jet stream velocity ($V_j = V_j(\max)_p$) is reached, the initial position of the pinion as the gear tooth chops the tail of the jet stream may be calculated from:

$$\theta_{p6} = m_g \theta_{g1} - \pi / N_p - \text{inv}\, \varphi + \text{inv}\, \varphi_{op} + 2\, B_p / N_p \tag{17}$$

(See Fig. 5.)

The final position at the point "A" in Fig. 6 is calculated from:

$$\theta_{op} = \cos^{-1}\left(\frac{r_s}{r_o}\right)$$

The maximum jet velocity may then be calculated from:

$$V_j(\max)_p = \frac{\omega_p[(R_o^2 - R_s^2)^{1/2} \sec \beta_p - (r_o^2 - r_s^2)^{1/2} \sec \beta_p]}{\theta_{p6} - \theta_{op}} \tag{18}$$

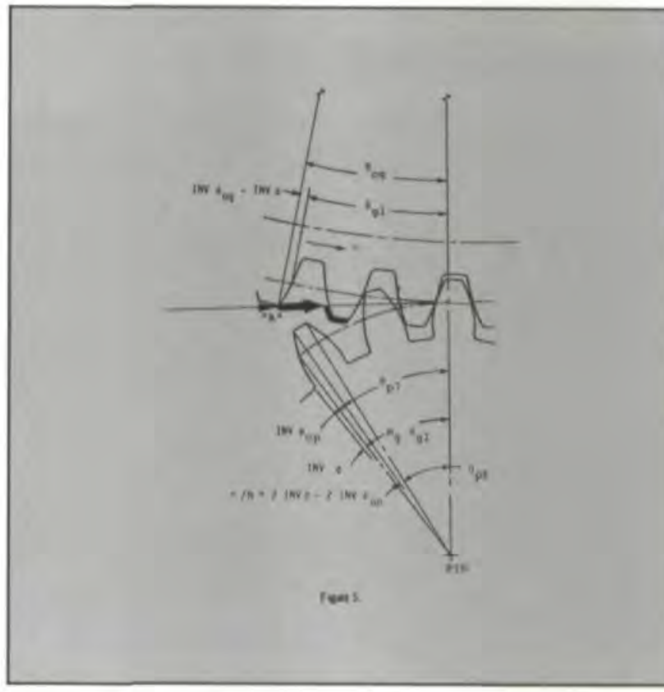

Figure 5.

Therefore, when $V_j \geq V_j(\max)_p$, $d_p = 0$, if $m_g > m_g(\text{crit})$. Also if $S = S_o$ and $\beta = \beta_p = \beta_{pp}$, then $V_j(\max)_p \to \infty$. $V_j(\max)_p = V_j(\text{Opt, U})$ then $V_j(\max)_p$ is set equal to $V_j(\text{Opt, U})$. Stated differently, when $V_j(\text{Opt, U})$ is greater than or equal to the calculated $V_j(\max)_p$, then $V_j(\max)_p$ no longer physically represents the solution, and $V_j(\text{Opt, U})$ is the maximum value that can be allowed for V_j.

Again, it should be noted that the selection or specification for V_j must be kept within the bounds of $\omega_p r \sec \beta_p$ and Equation 18 if impingement on the trailing side of the tooth profile is desired.

Equations 8 through 18 have been summarized in Table 1 on a velocity scale to add graphic visibility to their usability range.

The Gear — When the Jet Velocity is Greater than Pitch Line Velocity ($V_j > \omega_g R \sec \beta_p$).

The sequence of events for the gear in the case where $V_j > \omega_g R \sec \beta_p$ is shown in Figs. 5, 7 and 8. Again, instead of tracking the head, the trailing end or "tail" of the jet stream will be tracked after it is chopped at time ($t = 0$) as shown at "A" in Fig. 7, to the final impingement point at a depth "d_g" at time $t = t_\omega$, as shown in Fig. 8. The position of the pinion at time ($t = 0$) may be calculated from θ_{p3}, defined above. The associated gear position can be calculated from:

$$\theta_{g6} = (\theta_{p3}/m_g) + \text{inv}\,\varphi \tag{19}$$

which locates the gear at the time ($t = 0$) when the flight of the *tail* of the jet stream is initiated. (See Fig. 7.) The position of the gear when the jet stream *tail* is terminated on the gear may be calculated from:

$$\theta_{g7} = \tan^{-1}\left(\frac{L_g \cos \beta_p}{R + L_g \sin \beta_p}\right) + \text{inv}\,\varphi_{g7} \tag{20}$$

where

$$\text{inv}\,\varphi_{g7} = \tan \varphi_{g7} - \varphi_{g7}$$

$$\varphi_{g7} = \cos^{-1}\left(\frac{R_b}{[(R + L_g \sin \beta_p)^2 + (L_g \cos \beta_p)^2]^{1/2}}\right) \tag{21}$$

at time ($t = t_\omega$), as shown in Fig. 8.

Once again, when $0 \leq \beta_p < \beta_{pp}$ and $0 \leq S < S_o$, the *analysis* solution to the problem of cooling the gear is constrained by the jet velocity limits for the pinion to maintain impingement on same. And, as explained above, a given "gear mesh" must have a common jet velocity. Accordingly, a given impingement depth is selected for the pinion. Then, the associated jet velocity V_{jp} is solved for this velocity, which can then be used to find the associated gear impingement depth "d_g". Thus, after finding V_{jp}, solve for L_g iteratively from:

$$[(r_o^2 - r_s^2)^{1/2} \sec \beta_p - L_g]\omega_g = (\theta_{g6} - \theta_{g7})V_{jp} \tag{22}$$

and

$$d_g = R_o - [(R + L_g \sin \beta_p)^2 + (L_g \cos \beta_p)^2]^{1/2} \tag{23}$$

(continued on page 45)

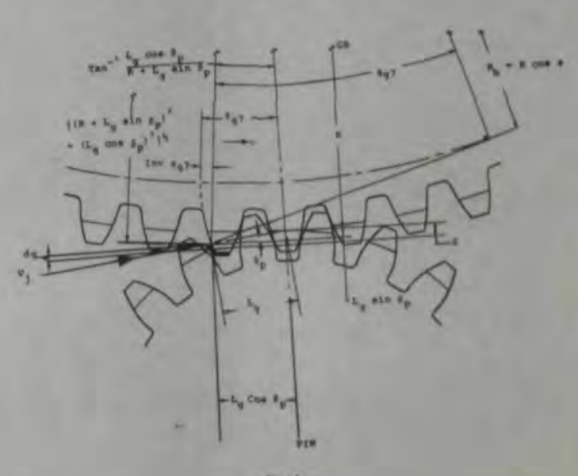

Back To Basics

Estimating Hobbing Times

Robert Endoy Ford New Holland, Inc.

Troy, MI

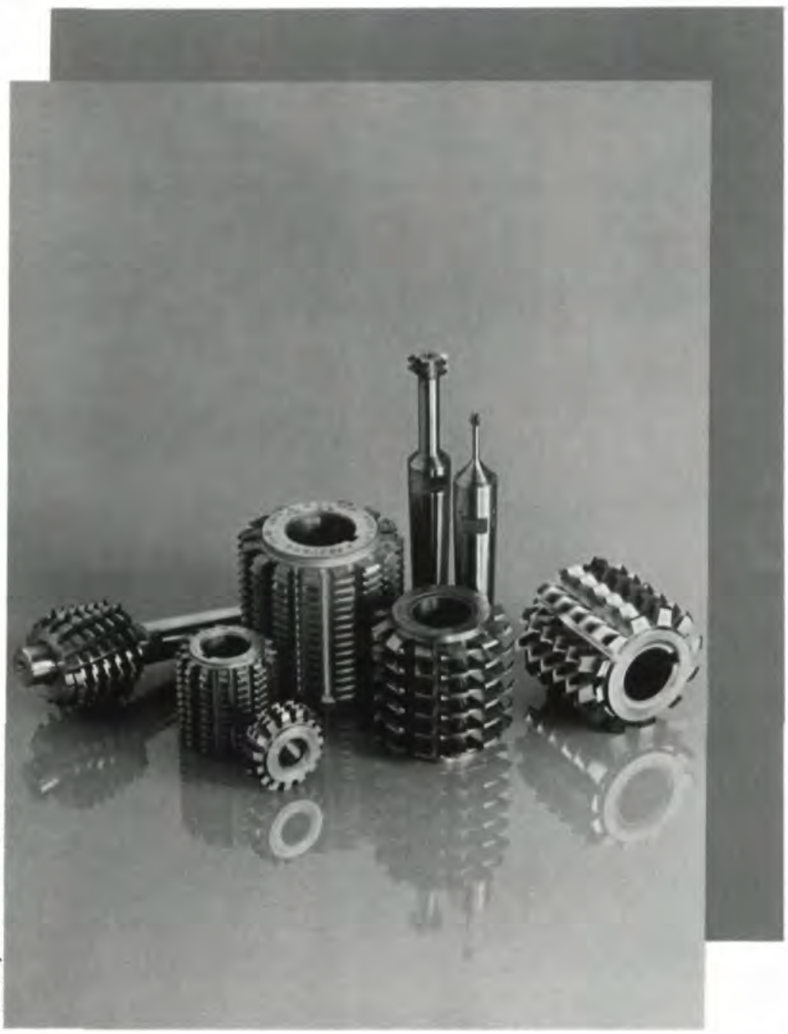

Courtesy of Mikron/Starcut Sales, Inc.

AUTHOR:

ROBERT ENDOY *is an advanced manufacturing planning engineer at Ford New Holland, Inc., working in the development, planning and launching of major tractor driveline programs. Prior to this work, he was with Hansen Transmissions International, Edegem, Belgium, and Ford Tractor Belgium. Mr. Endoy received a degree in industrial engineering from Hogere Technische School, Antwerp, Belgium, and is a Senior Member of the Society of Manufacturing Engineers.*

Hobbing is a continuous gear generation process widely used in the industry for high or low volume production of external cylindrical gears. Depending on the tooth size, gears and splines are hobbed in a single pass or in a two-pass cycle consisting of a roughing cut followed by a finishing cut. State-of-the-art hobbing machines have the capability to vary cutting parameters between first and second cut so that a different formula is used to calculate cycle times for single-cut and double-cut hobbing.

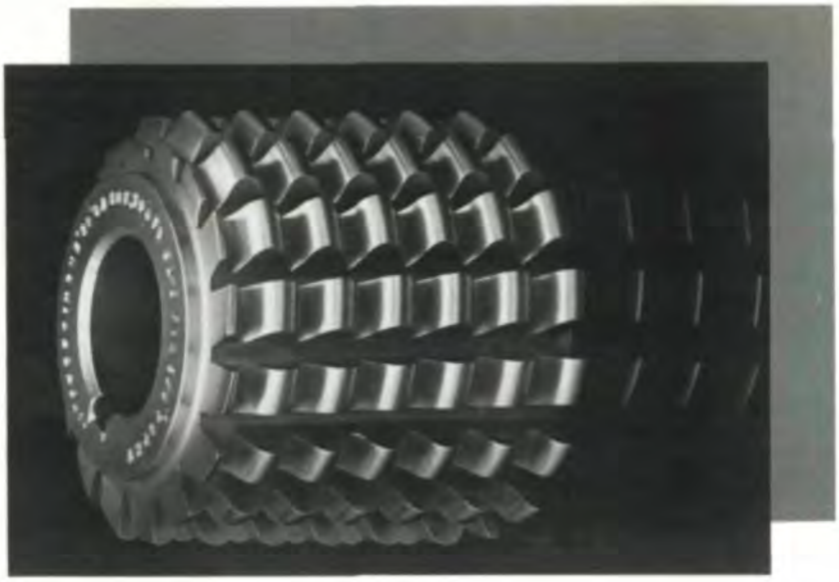

Single-Cut Hobbing Cycle

The cycle time is given by the equation,

$$T = \frac{Z \times L}{N \times K \times F} \qquad (1)$$

where

- T = cycle time in minutes
- Z = number of gear teeth
- L = length of cut in inches
- N = hob revolutions per minute
- K = number of hob starts
- F = feed rate in inches per revolution of work

Double-Cut Hobbing Cycle

The cycle time is given by the equation,

$$T = \frac{Z \times L1}{N1 \times K \times F1} + \frac{Z \times L2}{N2 \times K \times F2} \qquad (2)$$

where

- T = hobbing time in minutes
- Z = number of gear teeth
- L1 = hob travel in inches, first cut
- L2 = hob travel in inches, second cut
- N1 = hob revolutions per minute, first cut
- N2 = hob revolutions per minute, second cut
- K = number of hob starts
- F1 = feed rate in inches per revolution of work gear, first cut
- F2 = feed rate in inches per revolution of work gear, second cut

Some of the parameters of the cycle time formulae, such as the number of gear teeth, can be found directly on the part print. Others require additional calculations before they can be entered in the equation.

It is important to know that diametral pitch and pitch diameter of the work gear determine the size of the hobbing machine required for the job. The size of the gear tooth will also influence the feed rate that will be used to cut the gear, and whether the gear must be hobbed in a single- or double-cut cycle.

Calculation of Hob Travel (L)

The hob travel length consists of four elements: gear face width, spacer width, hob approach and hob overrun.

Gear Face Width. The gear face width is also indicated on the part print as the width of the gear blank. When more than one part is loaded per cycle, the total gear width must be taken into account. (Fig. 1)

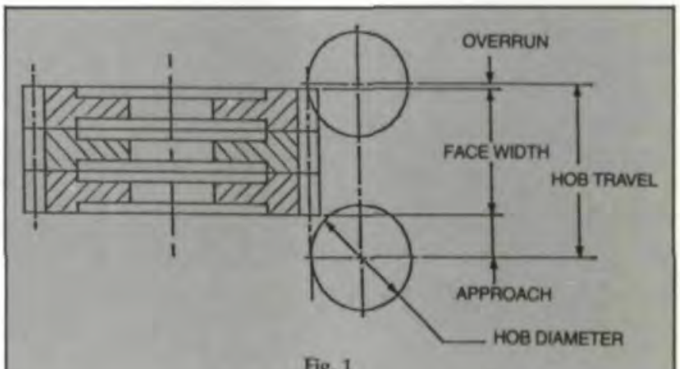

Fig. 1

Spacer Width. Gear configuration may be such that a spacer is required between gears in order to load more than one part per cycle. In this case the width of the spacer must be added to the total face width. (Fig. 2)

Approach. Hob approach is the distance from the point of initial contact between hob and gear blank to the point where the hob reaches full depth of cut. The approach length is a function of hob diameter, gear outside diameter, depth of cut and gear helix angle.

Hob approach is calculated with the formula

$$A = \sqrt{W \times \left[\frac{D + G - W}{\cos^2 (H)} - G\right]} \qquad (3)$$

where

A = hob approach in inches
W = depth of cut in inches
D = hob outside diameter in inches
G = gear outside diameter in inches
H = gear helix angle

For spur gears, $H = 0$ and $\cos H = 1$, so that the approach formula is simplified to

$$A = \sqrt{W \times (D - W)} \qquad (4)$$

Fig. 3 illustrates this relationship.

In a single-cut cycle the depth of cut is

$$W = \frac{\text{Gear outside dia.} - \text{Gear root dia.}}{2}$$

In a double-cut cycle the approach travel for roughing is longer than for finishing because of the difference in cutting depth. (Fig. 4)

Overrun. Hob overrun is the linear hob travel beyond full cutting depth required to complete generation of the gear teeth.

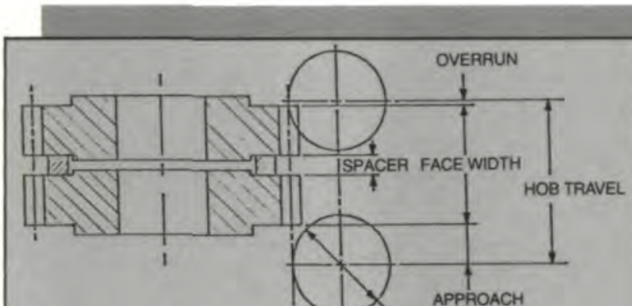

Fig. 2

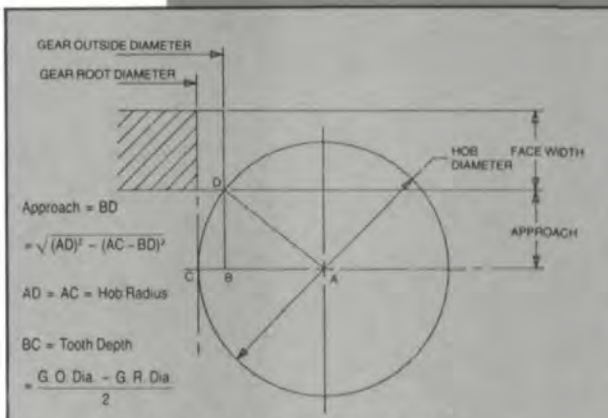

Fig. 3 – Hob Approach For Spur Gears

Hob overrun is calculated with the formula

$$R = \frac{S \times \cos (H) \times \tan (SA)}{\tan(PA)} \qquad (5)$$

where

R = hob overrun in inches
S = addendum of gear in inches
H = Gear helix angle
SA = hob head swivel angle
PA = gear pressure angle

The hob head swivel angle is a function of helix angle and hand of both work gear and hob.

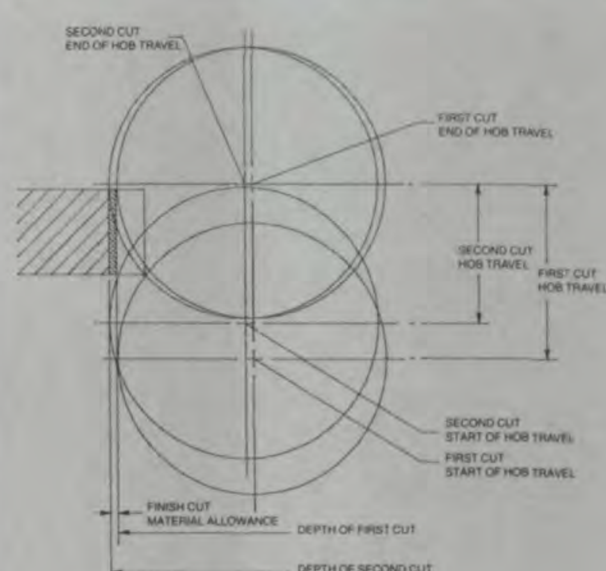

Fig. 4 – Hob Approach In A Two-Cut Hobbing Cycle

Table 1		
gear helix hand	hob helix hand	hob head swivel angle
left	left	H − HB
left	right	H + HB
right	left	H + HB
right	right	H − HB

In Table 1, HB represents the hob helix angle. The minimum hob head swivel angle is obtained when the helix of gear and hob have the same hand.

All formulae are based on the theoretical points of contact between hob and workpiece. In practice, clearance between hob and work gear is needed in order to assure safe cutting conditions. Therefore, a clearance amount of .040 to .100 inch must be added to the theoretical values of approach and overrun.

For spur gears, $H = 0°$; $\cos(H) = 1$; and $SA = HB$. For a 7 diametral pitch gear, with 20° pressure angle, and hobbed with a 3° helix hob, the overrun is

$$R = \frac{.1429 \times 0.05241}{0.36397} = 0.020$$

Obviously, for practical purposes the theoretical calculation of hob overrun for spur gears can be replaced by a fixed value which includes clearance, for instance, .100".

Hob Revolutions Per Minute (N)

Cutting speed in a hobbing operation is defined as the peripheral velocity of the hob.

$$V = \frac{\pi \times D \times N}{12} \tag{6}$$

where

V = Cutting speed in surface feet per minute (SFPM)
D = Hob diameter in inches
N = Revolutions per minute of the hob
π = 3.14159 . . .

In terms of machine set up, it is more significant to know the number of revolutions of the hob.

$$N = \frac{12 \times V}{\pi \times D} \tag{7}$$

As in most metal cutting processes, there are no specific values of speeds and feeds that must be used. Cutting parameters are, in fact, dependent on many variables, and starting values are often determined by past experience.

Speeds and feeds in an hobbing operation are affected by

- physical properties of tool material
- machinability of work material
- quality specifications
- ridigity of machine and fixture
- desired tool life
- cutting fluids, lubricants and coolants

Number of Hob Starts (K)

Number of hob starts and cycle time are inversely related to each other. Cycle time decreases when the number of hob starts is increased.

A single-start hob rotates the work one tooth for each revolution of the hob. With a 2, 3 or 4-start hob, the work is rotated over 2, 3 and 4 teeth for each revolution of the hob. Assuming the same feed rate for multistart as for single-start hobbing, the cycle will be completed 2, 3 or 4 times faster.

Quality considerations, however, limit the application of multistart hobs. In this process, fewer hob teeth participate in the generation of the tooth profile; therefore, it is less accurate. Multistart hobs also have an inherent thread spacing error which is repeated in the workpiece under certain conditions.

The following guidelines should be followed when estimating times with multistart hobs.

- The number of teeth in the gear must not be divisible by the number of hob starts.
- Only gears with a large number of teeth ($Z > 25$) are suitable for cutting with multistart hobs.

When working with multistart hobs the feed rate must be reduced to compensate for the increased tooth loading of the hob. The following reduction factors are recommended.

Table 2

Number of hob starts	Reduction factor
1	1
2	0.67
3	0.55
4	0.50

Example: Normal feed rate with single-start hob is .160" per revolution of workpiece.
When using a 2-start hob for the same job, the feed rate should be reduced to
$.67 \times .160 = .107$ inch/revolution.

Field of Application

Although hobbing is the most widely used method of gear manufacturing, its field of application is restricted by the part geometry. The major limitation is that hobbing is not applicable to internal gears. Other methods of gear manufacturing like shaping, broaching or skiving must be used for production of internal gears.

Another important limitation is that hobbing is not applicable to shoulder gears. This restriction is a direct result of the approach length, which is a function of the hob diameter. The distance between gear face and an adjacent shoulder must be greater than the minimum value of hob approach length in order to allow hobbing. In some cases it is possible to reduce the approach length by specifying hobs with reduced outside diameter. However, hob design considerations limit the variation in outside diameter.

Hobbing is without a doubt the most productive gear cutting method for external gears. It can be used as a semi-finishing or finishing gear process. Hobbing as a finishing process is accomplished by rough and finish cutting the gears on the hobbing machine without a subsequent tooth finishing operation. Most often hobbing is used in combination with a gear finishing operation like shaving or grinding.

Productivity can be increased by stacking several gears on the hobbing fixture. Stacks of more than two gears require good quality gear blanks with the gear rim faces parallel to each other and square to the bore.

One remarkable feature of the hobbing machine is the ability to make crowned or tapered gears. Crowning is often used in gear design practice to avoid end loading of the gear teeth. Taper hobbing can be used to compensate for uneven shrinkage in heat treatment.

Heat treated helical gears are typically affected by lead unwind, which is a change in helix angle after hardening. Lead angle variations are very easily compensated for on a gear hobbing machine by installing sets of differential change gears, or by programming of corrected helix angles on CNC controls.

EXAMPLES OF CYCLE CALCULATIONS

Example 1

Transmission gear hobbed on arbor fixture (Fig. 5)

Part print data

Number of teeth	61
Diametral pitch	7
Pitch diameter	8.714
Outside diameter max	8.990
Outside diameter min	8.985
Root diameter max	8.346
Root diameter min	8.336
Pressure angle	20°
Helix angle	0°
Face width	1.215
Material	SAE 8620

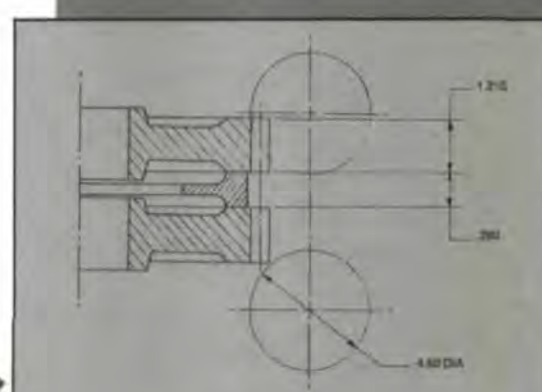

Fig. 5

Machine setting data

Double cut cycle	
Cutting speed rough	230 sfpm
Cutting speed finish	290 sfpm
Feed rate rough	.177 ipr
Feed rate finish	.236 ipr
Number of parts per cycle	2
Spacer width	.260
Finish cut material allowance	.060

Hob data

Outside diameter	4.60
Number of starts	1
Spiral angle	4.25°
Material	HSS

Cycle time calculation

$$\text{Hob rpm rough} = \frac{12 \times 230}{3.14159 \times 4.6} = 190 \text{ rpm}$$

$$\text{Hob rpm finish} = \frac{12 \times 290}{3.14159 \times 4.6} = 240 \text{ rpm}$$

$$\text{Gear addendum} = \frac{8.9875 - 8.7142}{2} = .137$$

$$\text{Whole tooth depth} = \frac{8.9875 - 8.341}{2} = .323$$

Depth of cut, roughing cut $= .323 - .060 = .263$

Depth of cut, finishing cut $= .060$

Hob approach, roughing cut $= \sqrt{.263 \times (4.60 - .263)}$
$= 1.068$

Add .040 clearance $= .040 + 1.068 = 1.108$

Hob approach, finishing cut $= \sqrt{.060 \times (4.60 - .060)} = .522$

Add .040 clearance $= .040 + .522 = .562$

$$\text{Hob overrun, rough and finish} = \frac{.137 \times \cos 0 \times \tan 3.25}{\tan 20}$$

$$= \frac{.137 \times .05678}{.36397} = .021$$

Add .040 clearance $= .040 + .021 = .061$

Total hob travel, roughing $= 1.068 + .061 + 2.430$
$+ .260 = 3.819$

Total hob travel, finishing $= .562 + .061 + 2.430 + .260$
$= 3.313$

$$\text{Cycle time} = \frac{61 \times 3.819}{190 \times .177} + \frac{61 \times 3.313}{240 \times .236}$$

$= 10.495$ min for 2 pieces

$= 5.297$ min for 1 piece

Example 2

The procedure is the same as in Example 1, however, the gear is now hobbed with a 2-start hob. We will assume that the 2-start hob has the same outside diameter as the single-start hob so that approach and overrun values are same as in previous example.

Feed rate for roughing $= .67 \times .177 = .118$

Feed rate for finishing $= .67 \times .236 = .158$

$$\text{Cycle time} = \frac{61 \times 3.819}{190 \times 2 \times .118} + \frac{61 \times 3.313}{240 \times 2 \times .158}$$

$= 7.859$ min for 2 pieces
$= 3.929$ min for 1 piece

The savings in cycle time is $10.495 - 7.859 = 2.636$ min or 25%.

This example illustrates clearly the increased productivity which results from the use of multistart hobs. ■

(continued from page 23)

In worm gears, the sliding induced by the rotation of the worm is greater than the sliding orthogonal to the lines of contact induced by the rotation of the gear wheel. It is essential that the simulator used to evaluate the pressure endurance curve be able to reproduce these components. Conventional roller machines could not be used.

The machine we designed consists of a disk that represents the worm, on which turns and slides a roller that represents the gear.

The axes of the disk and roller are perpendicular (Fig. 5).

It is possible, by adjusting the position of the roller with respect to the disk and the speeds of rotation of the disk and roller, to reproduce any sliding condition that can occur in worm gears.

The test piece is the roller made of the gear material (UE12P bronze, for example). It has the following characteristics:

diameter:	100 mm
transverse crowning radius:	250 mm
width:	25 mm

The disk used is 200 mm in diameter. It is made of ground case-hardened steel.

The speed of rotation used and the corresponding sliding velocity are

wheel:	420 rpm
disk:	855 rpm

giving a mean sliding velocity of 8 m/s.

Obtaining a representative pressure endurance curve for a given pair of materials requires between 7,000 and 10,000 hours of testing, equivalent to the destruction of 30 to 35 rollers. But this method is advantageous because it is faster than bench testing gears. Moreover, the cost of the test pieces and the running costs of the simulator are very low.

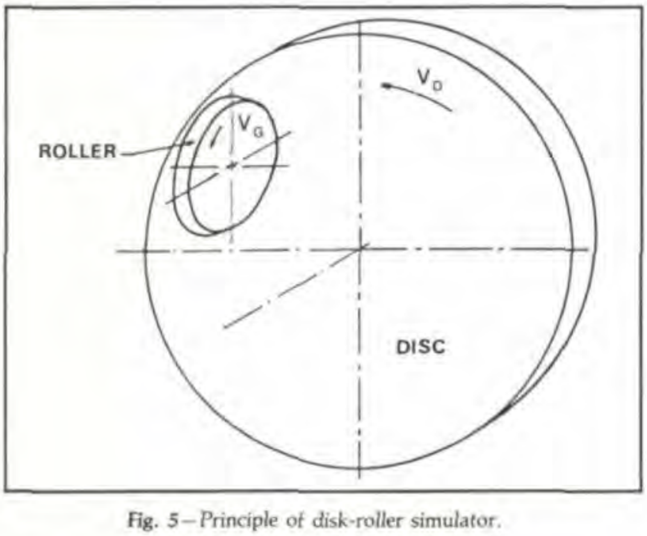

Fig. 5—Principle of disk-roller simulator.

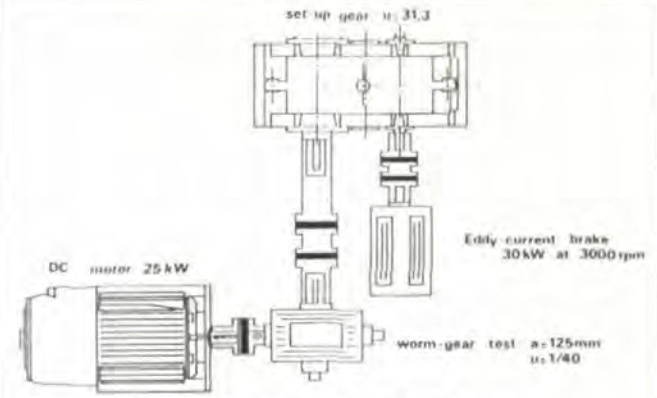

Fig. 6—Worm gear test bench.

Experimental Verification of the Design Method

For a complete verification of the design method, we carried out full-scale tests on worm gears. The test bench we built consists of a variable-speed DC motor that drives the worm of the reducer to be tested directly. The worm wheel at the reducer output is connected to a multiplier that drives an eddy-current brake, used to apply the load (Fig. 6).

The operation of the bench is monitored at all times and the following parameters are measured continually:

- the speed of rotation of the worm,
- the torque delivered by the motor,
- the torque applied by the brake,
- the oil temperature in the reducer housing,
- the temperature of the more heavily loaded worm bearing,
- the instantaneous wear of the test gear.

This last measurement is made by using a special device built by CETIM, based on the use of optical encoders (sensitivity 0.05 mm).

The test bench also has a lubrication system with oil circulation and cooling. The principle of this test bench is shown in Fig. 6.

Characteristics of the test gearing:

• number of threads:	1
• number of teeth:	40
• axial module:	4.95
• center distance:	125 mm
• helix angle:	5.5°
• face width of wheel:	45 mm
• axial pressure angle:	22°
• type of thread profile:	A

- synthetic oil
- worm made of case-hardened steel
- gear made of UE12P bronze

Application of the Design Method

The calculation model described below is contained in a program developed on the VAX 780. If we apply this method to the design of the test gear, we find:

- elasticity factor: ZE = 498
- *pressure distribution factor:* *ZR = 1693*

- integrated efficiency (calculated): $\eta = 0.62$
  (mineral oil)
- sliding velocity: 4.4 m/s
- speed of worm: 1600 rpm
- pitch diameter of gear: 198 mm

The measured efficiency was 0.8. The difference we found between the measured and calculated values comes from the fact that the efficiency was calculated on the basis of the "friction versus sliding velocity" curve taken from standard BS 721.

This curve is for a mineral oil, and the result it gives is low when the oil actually used is a synthetic oil with low-friction additives.

Fig. 7 shows the projection along the lines of contact on the flanks of the gear wheel of:

- the distribution of the equivalent radii of curvature;
- the distribution of the mean equivalent stiffness
- the distribution of the contact pressures.

It will be noted that the pressure distribution is to a first approximation the direct combination of the equivalent radii of curvature and the equivalent stiffness.

Comparison of the Results Obtained

The first experimental results obtained on these test benches now cover 12,000 hours for the disk and roller machine and 10,000 hours on the worm gear machine. The grades of materials used on these test benches are strictly identical.

Thirty rollers have been tested on the disk-roller simulator, yielding the pressure versus number of cycles curve given in Fig. 8. The pressure indicated on the y-axis corresponds to the Hertz maximum pressure obtained on the path, which is clearly visible after about four hours running.

The test gearing was subjected to a torque of 115 daN.m on the gear. The first pitting appeared on the flanks of the teeth after 3200 hours of tests, corresponding to $7.68\ 10^6$ loading cycles.

It should be noted that the surface damage found was located primarily at the roots of the gear teeth and on the meshing exit of the worm threads. This finding correlates perfectly with the pressure distribution maps given in Fig. 7.

Looking at the endurance curve obtained on the simulator, we find that $7.68\ 10^6$ cycles corresponds to an admissible pressure of 460 MPa (Fig. 8).

The calculation method, applied to this admissible pressure value, gives us the following transmissible torque:

$$C_r = 5.10^{-4}\cdot d_{w2}\cdot\eta\cdot\left(\frac{\sigma_{Hlin}}{ZE}\right)^2 .ZR =$$

$$C_r = 5.10^{-4} \times 198 \times \left(\frac{460}{498}\right)^2 \times 1693 \times 0.8$$

$$C_r = 114.4 \text{ daN.m}$$

This is very close to the value applied to the gear on the test bench.

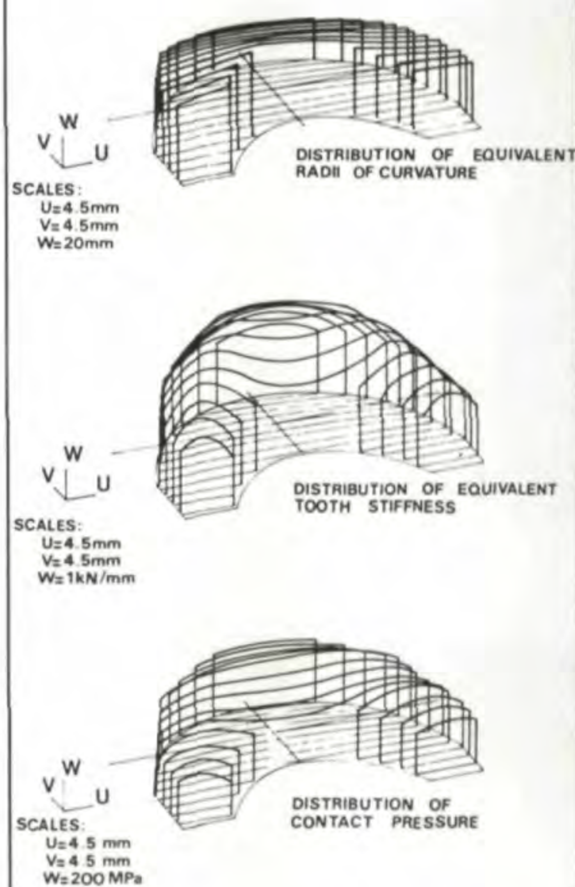

Fig. 7 – Distribution along contact line.

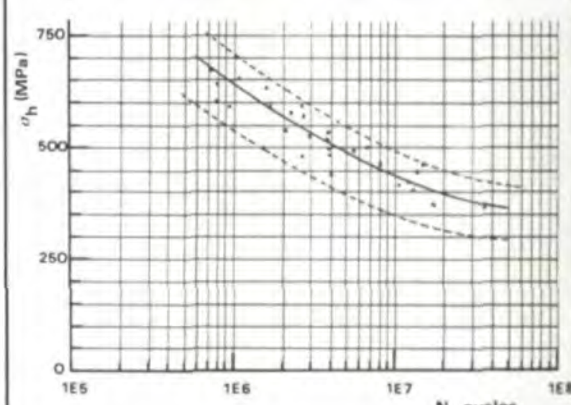

Fig. 8 – Pressure cycles curves for UE12P bronze.

VIEWPOINT

Dear Editors:

The magazine *Gear Technology* is praiseworthy. I keep every issue for reference.

The May/June issue that arrived today contained some typos in the mathematical equations that will cause incorrect answers. I'm confident that Mr. Ilya Bass submitted (or has) the correct equations, because his sample calculation resulted in the correct value for M_s.

In Equation 1 on page 26 and the equation for M_s near the top of the second column of page 28, the subscript "n" does not belong with the term inv ϕ. As written, the equation yields a result for the sample calculation that errs by more than 0.0052 inches.

Sincerely,

Evan L. Jones.
Gear Engineer
Chrysler Motors Corporation

Mr. Bass' response;

I can understand Mr. Jones' confusion. When I defined the values for Equation 1, I perhaps should have specified that M_s is the *spanned* measurement in the *normal* plane. The article is correct as printed.

Conclusions

The experimental results are in good agreement with the results yielded by the analytical design method. Other tests are now in progress to validate this new approach to the design of worm gears. Other materials are also being tested on our disk-roller simulator.

Appendix

UE 12 P bronze is a chilled cast bronze with 12% of tin and less than 1% of phosphor. It is equivalent to SAE 65 bronze.

References:

1. HENRIOT, G. *Theoretical and Practical Treated in Gearing* T1 & T2 – Ed. DUNOD Paris, 1979 (In French)
2. OCTRUE, M. and M. DENIS *Geometry of Worm Gears* Technical Note 22 – CETIM 1982. (In French)
3. OCTRUE, M. Analytical Method for Rating Worm Gears. Doctoral Thesis. – 1985. (In French)
4. OCTRUE, M. Software CADOR–ROUVIS – CETIM 1988 (In French)
5. OCTRUE, M., M. DENIS, and M. FAURE – "Rating Method For Worm Gears" 2éme CME – Paris 1986. (In French)
6. BS 721 – Specification for worm gearing – 1984
7. WILKESMANN, H. "Calculation of cylindrical worm gear drives of different tooth profiles" – *ASME Mechanical Design*, 1981, Vol. 103.
8. WEBER, C. "The Deformations of Loaded Gears and the Effects on Their Load-Carrying Capacity." British Dept. of Sci. and Indust. Research – Report n° 3, 1949.

ACKNOWLEDGEMENT: *Reprinted with permission of the American Gear Manufacturers Association. The opinions, statements and conclusions presented in this paper are those of the Author and in no way represent the position or opinion of the AMERICAN GEAR MANUFACTURERS ASSOCIATION.*

(continued from page 19)

CAD and Optimum Design

The design of an internal gearing is much more complicated than that of an external gearing. Computer aided design is recommended.[12] However, the following principles can also be used for external gearing design.

Mathematical Model. The first step is to analyze the specifications of the gearing and to construct a mathematical model that can simulate the problem to be solved. If the problem is restricted to geometrical dimensions only, usually efficiency or contact ratio can be chosen as the objective function. If the problem includes strength as well, the objective function can be chosen from one or two of the following variables: weight, size, output torque, efficiency, minimum stress, maximum strength, etc. The constraints are related to the data given. Sometimes the objectives and the constraints can be exchanged. For example, if the objective is the minimum size, the allowable stress or the maximum stress will be the constraint, and if the maximum strength is the objective, the given size or the minimum size will be the constraint. However, some parameters, such as different kinds of interference, may always be constraints. Both objective functions and constraint functions should be as simple as possible.

Optimizing Method. Since there are various parameters in a gearing design and the mathematic model is usually not a quadratic function or other well-behaved function, the author suggests not using indirect search techniques. These require both objective and constraint functions differentiable and continuous within the region of search, while the functions of a gearing are usually transcendental functions, the differentiation of which is sometimes very difficult. Therefore, it is recommended that the direct search techniques, such as the Hooke-Jeeves method, complex method, Rosenbrock method, all of which have been tested with good results in gear design by the author, be used. These methods have been introduced in many books.[14-15] However, they are analyzed as unconstrained problems, which might be common in mathematics; but most problems in engineering, including gear design, are constraint problems. Therefore, modifications of these methods should be made for a gear optimizing design, such as shown in Reference 12. Fig. 8 is a schemetic flow chart for a gear design. The program should be designed not for one cutter, but for a set of cutters. Different data can be obtained from different cutters from which the optimum result can be determined.

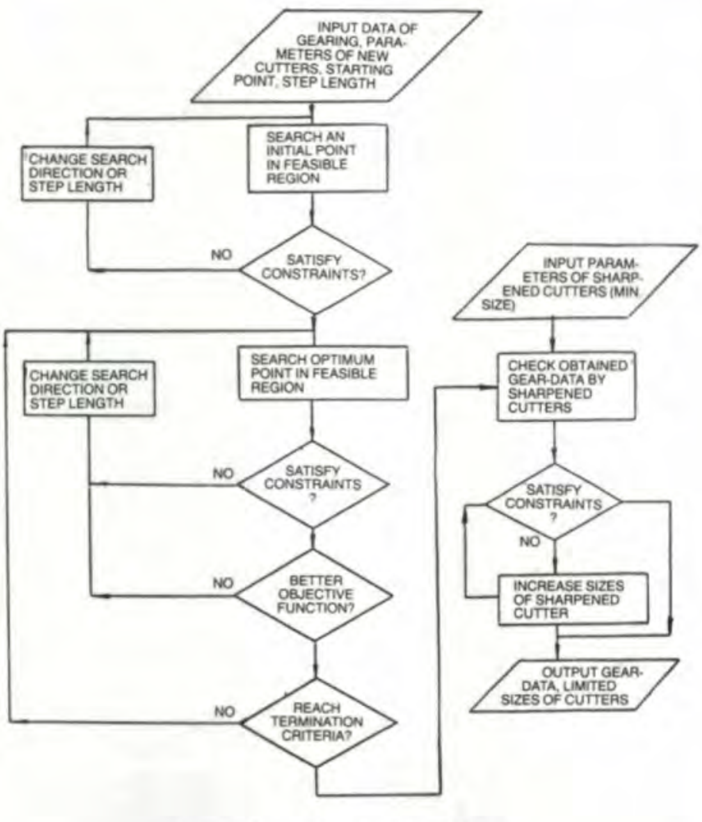

Fig. 8—Flow Chart for Gear Design.

Conclusion

As a result of the above discussion and the illustrative examples, the following observations can be made.

1). The method of gear teeth generation and the parameters of the cutter, including interference calculation, should be taken into account in the design of the internal gearing. Otherwise, the design seems correct, but, practically, there might be interference and other problems.

2). After choosing the cutter, use the parameters of a new cutter or the measured sizes of the cutter to design the gearing. Then use the minimum sizes of the cutter to check the obtained data. Otherwise, even if the parameters of the new cutter are taken into account, there might be interference when the gears are cut by the sharpened cutter.

3). The root radius of a gear is directly related to the parameters of the cutter. The two tip radii of a pair of gears have relation to interference, contact ratio, sliding velocity, top land, clearance, whole depth, etc. Some of them are related to root radii too. Hence, the tip radii have indirect relations with the cutter as well. But in many books (References 3, 5, 10, 16 and 17), the formulae for calculating the root radii or the tip radii have no relationship to the parameters of the cutters. The relation between the tip radius and the root radius of the external gearing is mainly for keeping a standard whole depth and a standard clearance. This method has been introduced to internal gearing for making the whole depth and the clearance close to standard values. (See Reference 3.) In some books,[10] the root radius is calculated from a given dedendum or addendum plus clearance. However, the author considers those methods improper because interference, contact ratio and other meshing indices are more important than the standard or the given whole depth. Besides, the root radius is determined by the parameters of the cutter, and the whole depth and the dedendum should be calculated from the root radius. Moreover, there might be few cases where an internal gear cut by a shaper cutter can obtain the standard or given whole depth. From Equations 7-9, only when $(X_2 - X_c) = 0$ will it be possible to cut a gear with the standard dedendum or a dedendum equal to the addendum of the cutter. If the addendum of the gear is standard, then the whole depth can be standard. However, the X_c is changing after sharpening and even during cutting. Therefore, the standard whole depth and the standard clearance are really of no meaning for the internal gearing. In Reference 18, the clearance can have a range, 0.25/P to 0.35/P. It is better than one value, 0.25/P, but the range should be larger because the clearance is of less importance, and sometimes even if it is 0.35/P, there will still be interference. In the above examples, none of the clearances or the whole depths are standard. Nevertheless, these designs satisfy the required indices and have been tested. For the internal gearing in the KHV planetary systems, if $N_2 - N_1 = 1$, the clearance usually should be greater than 0.5/P, and sometimes as large as 0.7/P. Hence, the author suggests that for internal gearing, the root radii be determined by "cutting" and the tip radii be determined by "meshing". Cutting means the parameters of the cutter. Meshing means meshing indices which are determined not by a single gear, but by the two mating gears. According to different requirements of different types of planetary gearings, choose one or two meshing indices, for example, contact ratio or transitional interference or clearance, to determine preliminary tip radii; then check other required indices. Since this discussion is mainly of interference, the details of the design for internal gearing will be in another article.

References

1. YU, DAVID D., NORMAN BEACHLEY, "On the Mechanical Efficiency of Differential Gearing", *Transactions of ASME, Journal of Mechanisms, Transmissions, and Automation in Design*, Vol. 107, Mar., 1985, pp. 61-67.
2. SIEGEL, MARTIN J., et al., *Mechanical Design of Machines*, International Textbook Co., 1965.
3. ROLOFF, HERMANN, *Maschinenelemente*, Friedr. Vieweg & Sohns, Braunschweig, 1966.
4. *Catalog*, Ishikawajima-Harima Heavy Industries Co., 1981.
5. DEAN, P. M., JR., Chapter 5 in *Gear Handbook*, Darle W. Dudley, ed., McGraw-Hill Co., 1962.
6. COLBOURNE, J. R., "Gear Tooth Interference", *Transactions of ASME*, Vol. 105, Sept. 1983, pp. 298-301.
7. DEUTSCHMAN, A. D., et al., *Machine Design*, Macmillan Publishing Co., 1975.
8. SHIGLEY, JOSEPH E., et al., *Theory of Machines & Mechanisms*, McGraw-Hill Book Co., 1980.
9. OBERY, ERIK, et al., *Machinery's Handbook*, 22nd Edition, International Press Inc., 1984.
10. DUDLEY, D. W., *Practical Gear Design*, McGraw-Hill Co., 1954.
11. SPOTTS, M. F., *Design of Machine Elements*, 6th Edition, Prentice-Hall, Inc., 1985.
12. YU, DAVID. D., "The Optimizing Programming Design of The KHV Planetary Gear Driving," *Proceedings of the International Symposium on Gearing and Power Transmissions*, Tokyo, 1981, pp. 295-299.
13. *Catalog*, Ash Gear & Supply.
14. KUESTER, JAMES L., et al., *Optimization Techniques with Fortran*, McGraw-Hill Book Co., 1973.
15. BEVERIDGE, GORDON S. G., et al., *Optimization*, McGraw-Hill Book Co., 1970.
16. KUDLYAVTZEV, V. H., *Machine Elements* (Russian), Machine Building Publishing House, 1980.
17. JIS(Japanese), 1973.
18. BOLOTOVSKAYA, T. P. *Geometrical Calculation for Involute Gear and Worm Transmissions* (Russian), Machine Building Publishing House, 1965.

Acknowledgement: This article was first presented at the 2nd World Congress on Gearing, March 3-5, 1986, Paris, France.

(continued from page 33)

TABLE 2. – EQUATIONS FOR OIL JET VELOCITY AND GEAR IMPINGEMENT DEPTH FOR PITCH LINE AND HIGHER OIL JET VELOCITIES

Relative velocity scale	Oil jet velocity	Pinion Impingement Depth
Critical high velocity to miss the gear	$V_j(\max)^*_g = \dfrac{\omega_g[(R_o^2 - R_s^2)^{1/2} - (r_o^2 - r_o^2)^{1/2}]\sec\beta_p}{\theta_{g1} - \theta_{g8}}$ $= V_j(\max)_p = \infty$, when $S = S_o$ and $\beta_p = \beta_{pp}$	$d_g(\min, U) = R_o - \{[R + L_g(\max)\sin\beta_p] + [L_g(\max)\cos\beta_p]^2\}^{1/2}$ *when $m_g \geq m_g(\mathrm{crit})$ <u>only</u> and $d_g(\min, u) = 0$ when $S = S_o$ and $\beta_p = \beta_{pp}$
Greater than pitch line velocity up to where the oil jet starts to miss the gear	$V_j = \dfrac{\omega_g\{(r_o^2 - r_s^2)^{1/2}\sec\beta_p - [(R_o - d_g)^2 - (R\cos\beta_p)^2]^{1/2} - R\sin\beta_p\}}{\theta_{g6} - \theta_{g7}}$ where $V_j(\min)_p \leq V_j \leq V_j(\max)_p$ V_j given	d_g given (usual design solution) $L = [(R_o - d_g)^2 - R^2\cos^2\beta_p]^{1/2} - R\sin\beta_p$ Iterate L_g from: $[(r_o^2 - r_o^2)\sec\beta_p - L_g]\omega_g = (\theta_{g1} - \theta_{g2})V_j$ then $d_g = R_o - [(R + L_g\sin\beta_p)^2 + (L_g\cos\beta_p)^2]^{1/2}$
Slightly higher and pitch line-upper end of velocity plateau	$V_j(\mathrm{opt}, U)_g = \dfrac{\omega_p(r_o - r_s)^{1/2}\sec\beta_p}{\theta_{p3}}$ $V_j = \omega_g R\sec\beta_p$(@ pitch point)	$d_g = a = \dfrac{1}{P_d} \pm \dfrac{\Delta N}{2P_d}$ (trailing profile) $d_g = a = \dfrac{(1 \pm \Delta N/2)}{P_d}$ (both profiles)

for $V_j(\mathrm{Opt}, U)_p < V_j < V_j(\max)_p$.

The *design* solution to the problem when $V_j(\min)_g < V_j < V_j(\max)_g$ may be calculated from:

$$V_j = \frac{[(r_o^2 - r_s^2)^{1/2}\sec\beta_p - \{(R_o - d_g)^2 - R^2\cos^2\beta_p\}^{1/2} + R\sin\beta_p]\omega_g}{\theta_{g6} - \theta_{g7}} \quad (24)$$

with the additional restriction that $V_j(\mathrm{Opt}, U)_g < V_j < V_j(\max)_g = V_j(\max)_p$. As for the others, Equation 24 is shown placed on the velocity scale of Table 2.

Also if V_j is specified within the range allowed for V_{jp} for Equation 8 and 24, then d_g can be calculated implicitly by solving iteratively for "L_g" from:

$$[(r_o^2 - r_s^2)^{1/2}\sec\beta_p - L_g]\omega_g = (\theta_{g6} - \theta_{g7})V_{jp} \quad \text{and} \quad (25)$$

$$d_g = R_o - [(R + L_g\sin\beta_p)^2 + (L_g\cos\beta_p)^2]^{1/2} \quad (26)$$

<u>When the Jet Velocity is Equal to Pitch Line Velocity ($V_j = \omega_g R\sec\beta_p$)</u>

Continuing up the velocity scale of Table 2 from $V_j = \omega_g R \sec\beta_p$, it can be shown that the upper limit for the constant impingement depth range, where $d_g = a$, can be calculated for the gear from:

$$V_j(\mathrm{Opt}, U)_g = \omega_p[(r_o^2 - r_s^2)^{1/2}\sec\beta_p \div \theta_{p3} \quad (27)$$

Thus, if the jet velocity V_j is between $V_j(\mathrm{Opt}, L)_g < V_j < V_j(\mathrm{Opt}, U)_g$, the impingement depth will be $d_g = a = 1/P_d$ on at least one side of the gear tooth profile. If $V_j = \omega_g R \sec\beta_p$ exactly, the d_p = "a" on both sides of the tooth profile.

Increasing the jet velocity above $V_j(\mathrm{Opt}, U)_g$ reduces the impingement depth d_g until $V_j = V_j(\max)_g$. When $S < S_o$, the tail of the jet chopped by the gear tooth is moving so fast as to be just missed by the pinion top land so that $d_p = 0$ and $m_g = m_g(\mathrm{lim.})$. When $S = S_o$ and $V_j(\max)_g \rightarrow \infty$, then $d_p \rightarrow 0$.

The initial position of the gear when it chops the tail of the leading jet stream is θ_{g1} as defined above when $m_g < m_g(\mathrm{crit})$

and as shown in Fig. 5 (for $S = 0$). The limit position "A" in Fig. 6 as the jet tail just misses the pinion top land is calculated from:

$$\theta_{g8} = (\theta_{p3}/m_g) + \pi/N_g + 2\,B_g/N_g \qquad (28)$$

$V_j(\max)_g$ in gear parameters may be calculated from:

$$V_j(\max)_g = \frac{\omega_g[(R_o^2 - R_s^2)^{1/2} - (r_o^2 - r_s^2)^{1/2}]\sec\beta_p}{\theta_{g1} - \theta_{g8}} \; (m_g \neq 1) \qquad (29)$$

Note that as $V_g(\max)_g \to \infty$ for $m_g \leq m_g(\text{crit})$ and when $m_g > m_g(\text{crit})$, then $V_j(\max)_g$ is finite at $d_p = 0$.

The impingement distance $L_g(\max)$ when $V_j = V_j(\max)_g$ may be iterated from:

$$\omega_g[(r_o^2 - r_s^2)^{1/2} \sec\beta_p - L_g(\max)] = (\theta_{g6} - \theta_{g7})V_j(\max)_g \qquad (30)$$

Then, when $S < S_o$

$$d_g = d_g(\min, U) = R_o - \{[R + L_g(\max)\sin\beta]^2 + [L_g(\max)\cos\beta]^2\}^{1/2} \qquad (31)$$

If $V_j(\max)_g \leq V_j(\text{Opt}, U)$ then set $V_j(\max)_g$ equal to $V_j(\text{Opt}, U)$. Also, it should be observed that since only one V_{jp} can be used, we must set Equations 18 and 29 equal: $V_j(\max)_p = V_j(\max)_g$ for the given m_g, making the design $m_g = m_g(\lim)$ when $m_g > m_g(\text{crit})$.

Summary

An analysis was conducted for into-mesh oil jet lubrication with an arbitrary offset and inclination angle from the pitch point for the case where the oil jet velocity is equal to or greater than pitch line velocity. Equations were developed for minimum and maximum oil jet impingement depths. The equations were also developed for the maximum oil jet velocity allowed, so as to impinge on the pinion and the optimum oil jet velocity required to obtain the best lubrication condition of maximum impingement depth and gear tooth cooling. The following results were obtained:

1. The optimum operating condition for best lubrication and cooling is provided when the jet velocity is equal to pitch line velocity $V_j = V_g \sec\beta_p = \omega_p r \sec\beta_p = \omega_g R \sec\beta_p$, whereby

both sides of the pinion and gear will be wetted, and the maximum impingement depth to the pitch line will be obtained.

2. When the jet velocity is slightly greater than the pitch line velocity, $\omega_p r \sec \beta_p < V_j < V_j(\text{Opt, U})$, the loaded side of the driven gear is favored and receives the best cooling with slightly less oil impingement than when $V_j = \omega_p r \sec \omega_p$.
3. As the jet velocity becomes much greater than the pitch line velocity, $V_j(\text{Opt, U}) < V_j < V_j(\max)_p$, the impingement depth is considerably reduced. As a result, the pinion may be completely missed by the lubricant so that no direct cooling of the pinion is provided when $V_j(\max)_p \leq V_j$.

References

1. AKIN, L., and TOWNSEND, D. "Cooling of Spur Gears with Oil Jet Directed into the Engaging Side of Mesh at Pitch Point", *JSME, Proc. of Inter. Symposium on Gearing and Power Transmissions,* Vol. 1, b-4, 1981, pp. 261-274.
2. TOWNSEND, D. and AKIN, L. "Study of Lubricant Jet Flow Phenomena in Spur Gears – Out-of-Mesh Condition", *Trans. ASME, J. Mech. Design,* Vol. 100, No. 1., Jan. 1978, pp. 61-68.
3. HEIJNINGEN, G.J.J. VAN and BLOK, H. "Continuous as Against Intermittent Fling-Off Cooling of Gear Teeth", *Trans. ASME Journal of Lub. Tech.,* Vol. 96, No. 4, Oct. 1974, pp. 529-538.
4. AKIN, L., MROSS, J., and TOWNSEND, D. "Theory for the Effect of Windage on the Lubricant Flow in the Tooth Spaces of Spur Gears", *Trans. ASME, J. Eng'rg. for Industry,* Vol. 79, Ser. B, No. 4, 1975, pp. 1266-1273.
5. AKIN, L. and TOWNSEND, D. "Study of Lubricant Jet Flow Phenomena in Spur Gears", *Trans ASME, J. Lubrication Tech.,* Vol. 97, Ser. F, No. 2, 1975, pp. 283-288.
6. TOWNSEND, D. and AKIN, L. "Analytical and Experimental Spur Gear Tooth Temperature as Affected by Operating Variables", *1980 Trans. J. Mech, Design,* ASME, Vol. 103, No. 4., Jan. 1981, pp. 219-226.
7. TOWNSEND, DENNIS P. "The Applications of Elastohydrodynamic Lubrication in Gear Tooth Contacts", NASA TMX 68142, Oct. 1972.
8. AKIN, L.S. and TOWNSEND D.P. "Into Mesh Lubrication of Spur Gears and Arbitrary Offset, Part I – For Oil Jet Velocity Less Than or Equal To Gear Velocity", *Gear Technology,* Vol. 6, No. 3, May/June, 1989, p. 30.

Acknowledgement: *Reprinted courtesy of American Society of Mechanical Engineers, from their Winter Annual Meeting, Phoenix, AZ, November 15-19, 1982, and ASME* Journal of Mechanisms, Transmisions, and Automation in Design, *Vol. 105, Dec., 1983, pp. 713-724.*

ADVERTISERS' INDEX

The advertisers listed below will have booths at Gear Expo '89.

Booth No. 301
AMERICAN PFAUTER CORP.
925 Estes Avenue
Elk Grove Village, IL 60007
(312) 640-7500

Booth No. 125
CIMA U.S.A.
501 S. Lake Blvd.
Richmond, VA 23235
(804) 794-9777

Booth No. 507
FUKUYAMA & ASSOC.
3340 San Marcos Dr.
Brookfield, WI 53005
(414) 781-4245

Booth No. 335
GMI MUTSCHLER
P.O. Box 193
Clarendon Hills, IL 60514
(312) 986-0756

Booth No. 420
GEAR TECHNOLOGY
P.O. Box 1426
1425 Lunt Avenue
Elk Grove Village, IL 60007
(312) 437-6604

Booth No. 236
GUEHRING AUTOMATION, INC.
P.O. Box 125
W227N6193 Sussex Road
Sussex, WI 53089
(414) 246-4994

Booth No. 120
ITW ILLINOIS TOOL WORKS
3601 W. Touhy Ave.
Lincolnwood, IL 60645
(312) 675-2100

Booth No. 234
JAMES ENGINEERING
11707 McBean Dr.
El Monte, CA 91732
(818) 442-2898

Booth No. 101
KLINGELNBERG AMERICA CORP.
P.O. Box 36926
15200 Foltz Industrial Pkwy.
Strongsville, OH 44136
(216) 572-2100

Booth No. 213
M & M PRECISION SYSTEMS
300 Progress Road
West Carrollton, OH 45449
(513) 859-8273

Booth No. 311
MITSUBISHI HEAVY INDUSTRIES LTD.
873 Supreme Drive
Bensenville, IL 60106
(312) 860-4220

Booth No. 237
MULTI-ARC SCIENTIFIC COATINGS
200 Roundhill Drive
Rockaway, NJ 07866
(201) 625-3400

Booth No. 543-45-47
NORMAC, INC.
P.O. Box 69
Airport Road Ind. Park
Arden, NC 20704
(704) 684-1002

Booth No. 114-116
OERLIKON-BÜHRLE LTD.
Birchstrasse 155
8050 - Zurich, Switzerland
Phone 01/316 22 11

Booth No. 301
PFAUTER-MAAG CUTTING TOOLS
P.O. Box 2950
1351 Windsor Road
Loves Park, IL 61132
(815) 877-0264

Booth No. 201
STARCUT SALES, INC.
P.O. Box 376
23461 Industrial Park Dr.
Farmington Hills, MI 48332-0376
(313) 474-8200

Booth No. 236
TRI-STATE MOTOR TRANSIT CO.
P.O. Box 113
Joplin, MO 64802
(800) 641-7582

FORMASTER
GRINDING WHEEL PROFILER

EASY TO INSTALL — Because of its small size and weight, the **FORMASTER** does not require major machine modifications and can be installed on nearly any grinder. Installation can usually be accomplished in less than a day.

EASY TO OPERATE — Two axis design simplifies programming and operation. You can choose between four popular controls that feature menu and G-Code programming, graphic simulation, automatic corner rounding, automatic diamond thickness compensation, and more.

IMPROVES ACCURACY

MADE IN U.S.A.

REDUCES WHEEL DRESSING TIME

Patent No. 4,559,919

ACCURATE — To within ± .0001″ of programmed dimension, with repeat accuracy to within .00006″. Extra precision roller bearing ways, pre-loaded roller screws and optical linear encoders, as well as superior design and construction, give the **FORMASTER** the ability to hold inspection gage accuracy.

PRODUCTIVE — No templates or special diamond rolls are needed, so lead times and tooling inventories are reduced. Most forms can be programmed and dressed in, ready to grind in 30 to 45 minutes. Refreshing the form between grinding passes is accomplished in seconds.

VERSATILE — Can be used with single point diamonds or with optional rotary diamond wheel attachment. Nearly any form can be dressed quickly, easily and accurately.

DURABLE — Hard seals are closely fitted and are air purged to totally exclude contamination. Sealed servo motors, automatic lubrication and totally enclosed encoders minimize down time and ensure long service life.

P.O. Box 69
Arden, NC 28704
(704) 684-1002

NORMAC

P.O. Box 207
Northville, MI 48167
(313) 349-2644

CIRCLE A-27 ON READER REPLY CARD